August 2005
Master's Thesis

A Study on the Bulbous Bow Design for Ultra Large Container Ship

Graduate School of Chosun University

Department of Naval Architecture & Ocean Engineering

E.S Sarath

A Study on the Bulbous Bow Design for Ultra Large Container Ship

초대형 컨테이너선의 구상선수 설계

August-2005

Graduate School of Chosun University

Department of Naval Architecture & Ocean Engineering

E.S Sarath

A Study on the Bulbous Bow Design for Ultra Large Container Ship

Advisor: Prof. Lee, Kwi Joo

Thesis Submitted for the degree of Master of Engineering

April-2005

Graduate School of Chosun University

Department of Naval Architecture & Ocean Engineering

E.S Sarath

Thesis submitted in partial fulfillment
of the requirement for the Award of
the degree of
Master of Engineering

Approved by the Guidance Committee:

Dr. Igor Shugan,
Chosun University _____

Professor Lee, Kwi Joo,
Chosun University _____

Professor Yoon, Duck Young,
Chosun University _____

May-2005

Graduate School of Chosun University

Contents

List of Figures

List of Tables

Nomenclature

C_A	:	Model-Ship Correlation Allowance
C_F	:	Frictional Resistance Coefficient
C_R	:	Residual Resistance Coefficient
C_T	:	Total Resistance Coefficient
R_N	:	Reynolds Number
F_N	:	Froude Number
K	:	Wave Number
u	:	X Direction Velocity Component
v	:	Y Direction Velocity Component
r_b	:	Bulb Radius
ς	:	Wave Height
ϕ	:	Potential Function
$\varPsi$	:	Stream Function
R	:	Mitchell's Wave Resistance
C_{ABT}	:	Bulb Cross sectional Parameter
C_{ZB}	:	Bulb Nose Height Parameter
C_{BB}	:	Bulb Breadth Parameter
C_{LPR}	:	Bulb Length Parameter
C_{ABL}	:	Bulb Lateral Parameter
C_{VPR}	:	Volumetric Parameter
R_V	:	Viscous Resistance
R_F	:	Frictional Resistance
R_{VR}	:	Viscous Residual Resistance
R_{WF}	:	Wave-making Resistance
R_{WB}	:	Wave-breaking Resistance
P_D	:	Delivered Power

초대형 컨테이너선의 구상선수 설계

Sarath E.S
지도 교수 : 이 귀 주
조선대학교 일반대학원
선박해양공학과

초 록

최근 조선시장은 고부가가치 선박인 컨테이너선박의 수요가 급증함에 따라 이에 대한 연구가 활발히 이루어지고 있다. 현재 설계되어진 컨테이너선은 9200TEU 로써 앞으로는 이보다 더 큰 용적의 컨테이너선의 수요가 있을 것으로 예상된다. 이에 따라 본 연구에서는 9,200TEU 선을 모선으로하여 주요요목을 결정하고 12,500TEU 선을 CAD 를이용하여 설계하였다. 이때 구상선수의 형상을 다르게 하여 구상선수 형상이 저항성능에 미치는 영향을 연구하였다. 1

구상선수 설계는 “Kracht Parameters”를 근거로 하여 nabla 타입 bulb 를 설계하고 그 다음에 nose height 와 area 별로 바꾸어 총 6 가지로 설계하였다. Kelvin's Wedge 이론 및 Ray 이론 그리고 CFD Code 를 이용하여 이론계산을 수행하여 wave pattern, wave height, 저항값을 얻을 수 있었다. 여기서 Kelvin's Wedge 이론 및 Ray 이론은 2-D 로 해석하였으며 CFD Code 중 하나인 Shipflow 는 3-D 로 해석하였다. 이와 같은 연구를 수행하여 얻은 결과를 비교 분석하여 12,500TEU 컨테이너선의 최적 구상선수를 설계하는데 목적을 두었다.

Bulb Design for Ultra Large Container Ship

Sarath E.S
Adv. Prof. Lee, Kwi-Joo
Dept. of Naval Architecture &
Ocean Engineering
Graduate School, Chosun University

ABSTRACT

In the outset, the paper envisages the current feasibility studies on the next generation Ultra Large Container Ship (ULCS) Design and its hydrodynamic aspects in a classical view point. Pressing demand for increased sizes and general consensus on the safety of Container ships are the motivations for this design. Current study focuses on the Hydrodynamic aspects of incorporating an ideal bulb for the mammoth ship with a capacity of 12500 TEU. Implementing ray theory clubbed with Kelvin's Wedge theory for the numerical analysis has derived a compromising results and pretty new idea formation for the design. The content of the paper will includes examination of design challenges, optimal design of hull form from hydrodynamic point of view, investigative studies on ideal bulb types and the numerical and CFD analysis for finding an ideal bulb for the hull form designed. Complying to the current market study on container shipment along with the necessity of maintaining high speeds stress on the necessity of optimizing the mammoth hull form for the ship with a potential bulb shape. Ray theory, evolved as an extension to the linear wave theory evolved as a proper tool for the design and has proved to give a satisfactory result with sufficient precision. A feedback check using CFD coding gives better results in wave pattern generated by the bow waves and a close check on caustics nullify the probability of wave breaking. Broadly speaking, this paper highlight the ideal design prospects of an optimum bulb for the next generation ULCS.

CHAPTER 1

INTRODUCTION

1.1 Background

Recent years witnessed considerable increased in the sizes of Container Ships being built round the world. General consensus reiterates the inherent demand in the container shipping arena as well as the lucrative trade solutions blended with container trading are the basic motivating factors that compelled the ship owners to go for mammoth sizes of container ships. Container ships having a reputation of speedy transport and the relentless safety record won the faith and confidence of both ship owners as well as ship builders to redefine the shape and capacity of Container Ships to “Ultra Large Container Ships” (ULCS). Studies by expert naval architects round the world expressed their strong point of considerable reduction in Operational and Transportation cost per container unit carried at a design speed more than 23 knots. Broadly speaking, the concept to put to reality employs great deal of positive outlook from technological point of view as the ship’s size will grow mind boggling. Since the introduction of containerization over 40 years ago, the size of container ships has increased dramatically. Until the mid-1980s, size was limited by the dimensional constraints of the Panama Canal (principally, 32.2-metre beam). Since then, the development of the post-panamax fleet has been dramatic; today 30% of the world’s fleet, by capacity, is post-panamax. The largest of the ships currently on order have capacities of more than 8,000 TEU, and there is clearly scope for even larger ships. The demand for containerization, however, continues unabated, and it is this rapid demand growth which is underpinning the vast amount of new tonnage currently being ordered.

The trend is expected to continue for some time yet, albeit with some peaks and troughs as the market responds to variations in new build prices and availability of building slots

This new concept yet to be moved to the yard for building over 10000 TEU will have a fine fore and aft body with fuller midship section maintaining a service speed of more than 23 knots. Prediction of the basic dimensions of the next generation of ultra-large container ships must commence with an understanding of the current and anticipated future capabilities of the infra-structure with which these ships must interface. It is nonsense to consider the ships in isolation; they must be considered as part of a complete intermodal transport process. This is a necessary change of philosophy from previous generations when the ships could be designed to provide optimum performance at sea, knowing that the terminals could provide whatever capacity and capability was required to service the vessels during their brief periods in port.

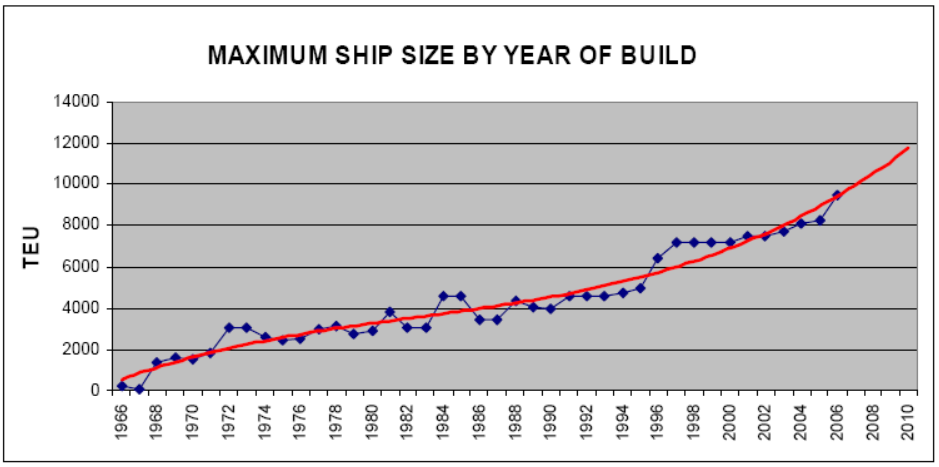

Fig 1.1 Extrapolation of the future Container Capacity

The actual maximum vessel size will be determined by the interplay between what can be constructed and what can be propelled at the required speed and what can be handled

effectively by the container terminals. The increase in main dimensions of the vessel in relation with the cost reduction is not yet reached the culminating point and hence more cumulative efforts can be expected for more sizes. Major infrastructural constraints bound to the ULCS are the container terminal capacity, draft restrictions in ports, range of cargo handling devices abreast the ships and repair yard facilities round the world.

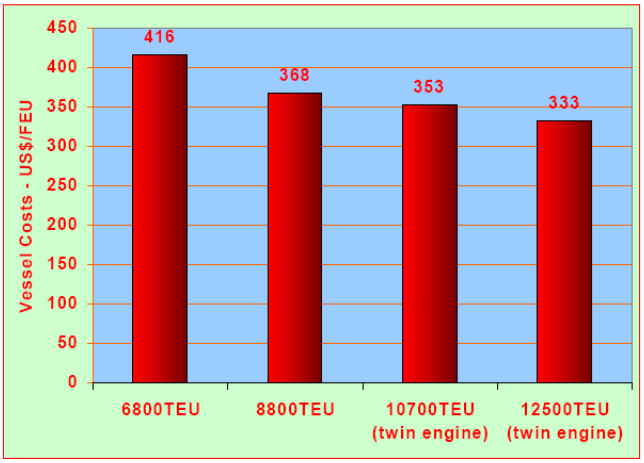

Fig 1.2 Economic Comparisons at 25 Knots

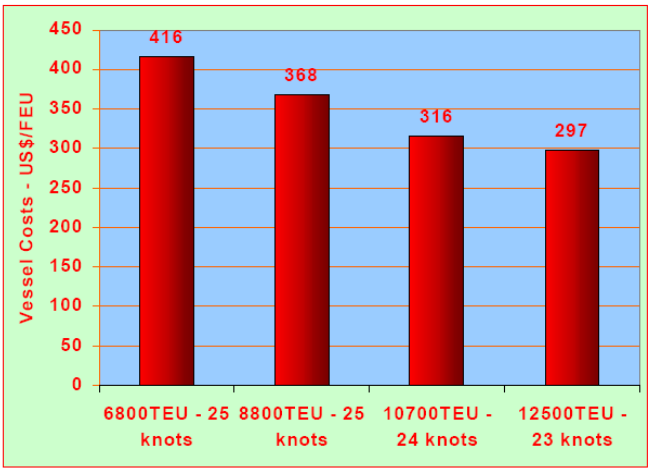

Fig 1.3 Economic Comparisons at 25 Knots

Environmental considerations outlook the current trend in shipbuilding as the classification societies and IMO impose strict restrictions in the performance of the ship from eco-stand point. Hence the necessity to adapt to the concept of green ship stands for the pin point study on the fuel consumption per container unit transported and the global marine transportation along with the ship. This new concept design will have a broad outlook as experts round the world see this as a gigantic ship of mind boggling volume and the success of the cutting edge technology employed. A close and well-defined design updated to modern shipyard facilities and class rules will be the key to the triumph of ULCS. ULCS class container ships are having a promising future ahead overcoming economic and technical challenges that the design, construction and operation of this new venture will meet with.

1.2 Motivation for the Study

Due to the current challenges and competition among the various shipyards round the world in search of an optimum hull form with excellent performance and the growing size of container ships attains importance for the study. Already the research works are already on in Scandinavian countries and in the Far East proving an extra edge to the concept study. An optimized bulb shape can remarkably reduce the total resistance and can impart excellent sea keeping and high speed characteristics. Hence, the purpose of the study is to find and analyze suitable bulb shape for conceptual ULCS theoretic cally and counter check by CFD.

1.3 Flowchart of the Design

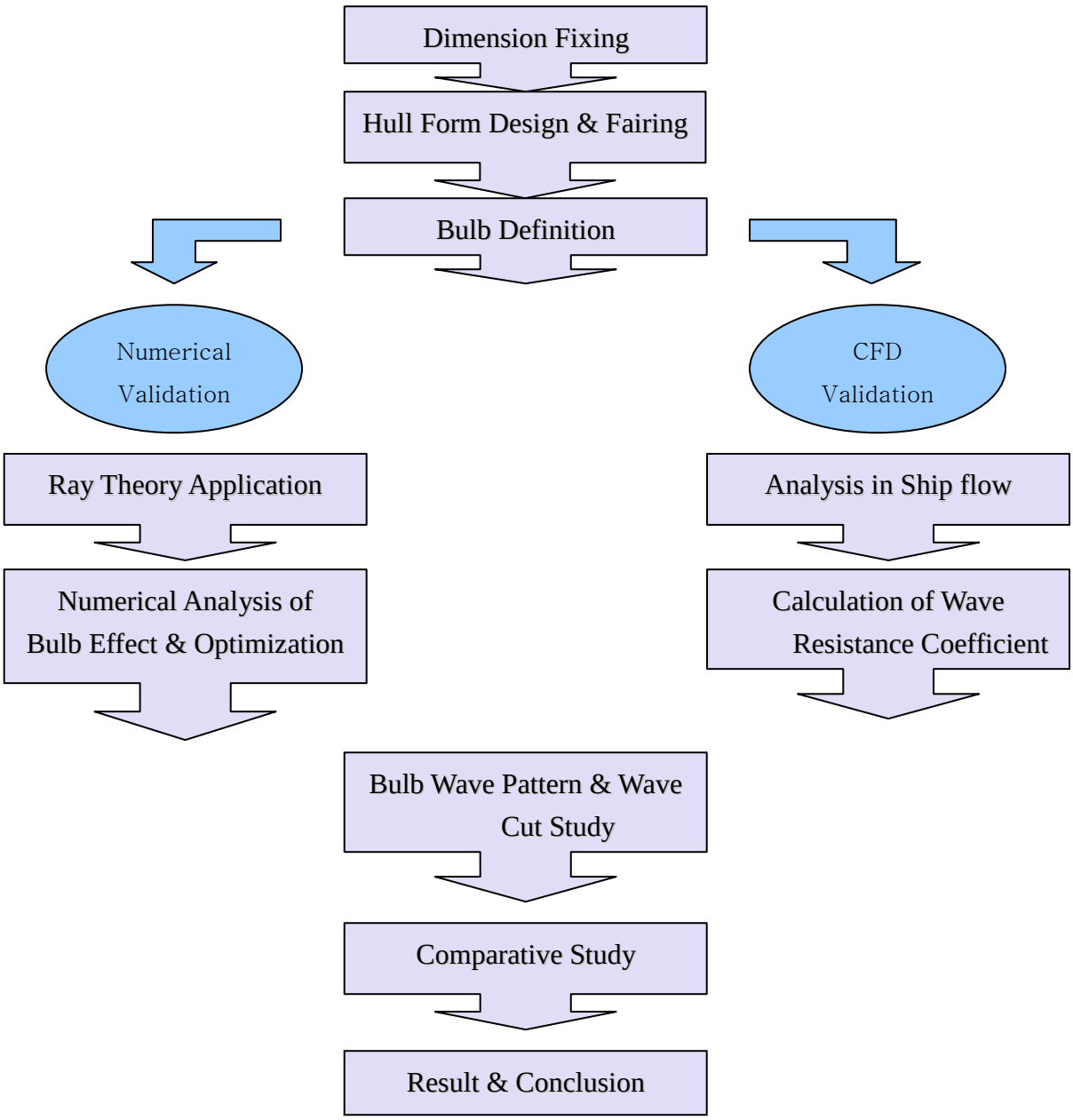

CHAPTER 2

HULL FORM DESIGN

2.1 Fixing of Main Dimensions

Container ships are designed as linear dimension ship. The dimensions are multiples of the containers being stowed. Draft and breadth restrictions in the areas where she ply also impose limitations in design. Parent ship analysis reveals that most of the ships carry 45% of the containers under deck. Containers are susceptible to severe stability problems due to her fine hull form. Hence she is designed to carry 15 – 20 % permanent ballast.

Container Specifications

Length	6.096 m
Width	2.438 m
Height	2.438 m

Capacity

Internal cubic capacity	31.04 m^3
Maximum load capacity	20.3 t
Weight of empty container	2.25 t

Total capacity = 12500 TEU

Analyzing the parent ship data [8], it is decided to carry 45% of the total containers under deck. Therefore the number of containers to be carried under deck,

N_{CU} = $(45 \times 12500) / 100$ = 5625

The arrangement of containers in the midship under deck is taken as 20 x 9 and above deck is determined as 22 x 7. The breadth and depth are subsequently determined.

Hence, the total number of files (Bays) to be stacked in the longitudinal direction,

N_f = $Ncu \times f /(Nr \times Nt)$

Where, f = 1.1 to 1.25

= 1.25 (chosen)

N_f : Number of files

Nr : Number of rows

Nt : Number of tiers.

N_f = 5625 x 1.25 / (20×9)

= 39.06 ~ 40 files

2.1.1 Estimation of Length

By Container Stowage

From the number of files calculated, the length between perpendiculars can be calculated providing sufficient clearances in the longitudinal directions and considering the space

requirement for the cargo hold, engine room, fore peak and aft peak tanks. Approximating the length of aft peak (3.5% of Lbp) and fore peak (5% of Lbp), with the length of the engine room 12 - 15% of the total length,

L_{BP} = $N_f \times (6.096 + 1.0) / [1 – (0.035+0.05+0.15]$ = 371 m

2.1.2 Estimation of Breadth

Container ships normally have the hatch opening width 80% – 85% of the total breadth of the vessel for fast cargo handling.

B = (2.438 x 22) + (21 x 0.12)

B = 56.2 m

Breadth of the Container : 2.438 m

Clearance between the Containers : 0.12 m

Hence, Breadth, B = 56.2 m (Selected)

2.1.3 Estimation of Depth

D = $Nt \times$ (2.438+0.025) + Hdb + GAP – H_{HC}

N_t = Number of tiers.

H_{DB} = Double bottom height. Min.value is $28 \times B + 205 \times \sqrt{T}$ [12]

= 2354.2 mm (for T = 14.5, assumed)

= 2.4 m (selected)

GAP = Allowance at top between containers and hatch cover

= 0.5 m (taken)

H_{HC} = Hatch coaming height

= 1.5 m (minimum height required is 0.76 m)

D = 9 × (2.438+0.5) + 2.4 + 0.5 - 1.5

Hence, Depth, D = 28 m

2.1.4 Form Coefficients

Block Coefficient (C_b)

Froude number = $V / \sqrt{(gL)}$

= 0.213

C_B = $1.06-1.68 F_N$ Ayres formula [11]

= 0.69

Midship Area Coefficient (C_m)

C_M = $0.9 + 0.1 C_B$ = 0.969 VanLammerin [11]

Water Plane Area Coefficient (C_w)

C_W = $0.76 C_B + 0.273 = 0.797$

Prismatic Coefficient (C_p)

$$Cp = C_B / C_M = 0.712$$

Draft for container ships is found by optimizing all other main particulars of the vessel and the iteration with deadweight and is calculated as 14.5 m complying with all port depth restrictions.

2.2 Hull Form Drawing

The hull form is designed form a parent ship hull of a 8600 TEU Single Screw vessel with almost same block coefficient. The hull is characterized by large flare angle at bow with fuller midship section and full breadth transom with 8m over hang. The hull is faired to fit the bulbs with close approximations in AutoCAD. The body plan developed for the purpose is shown below.

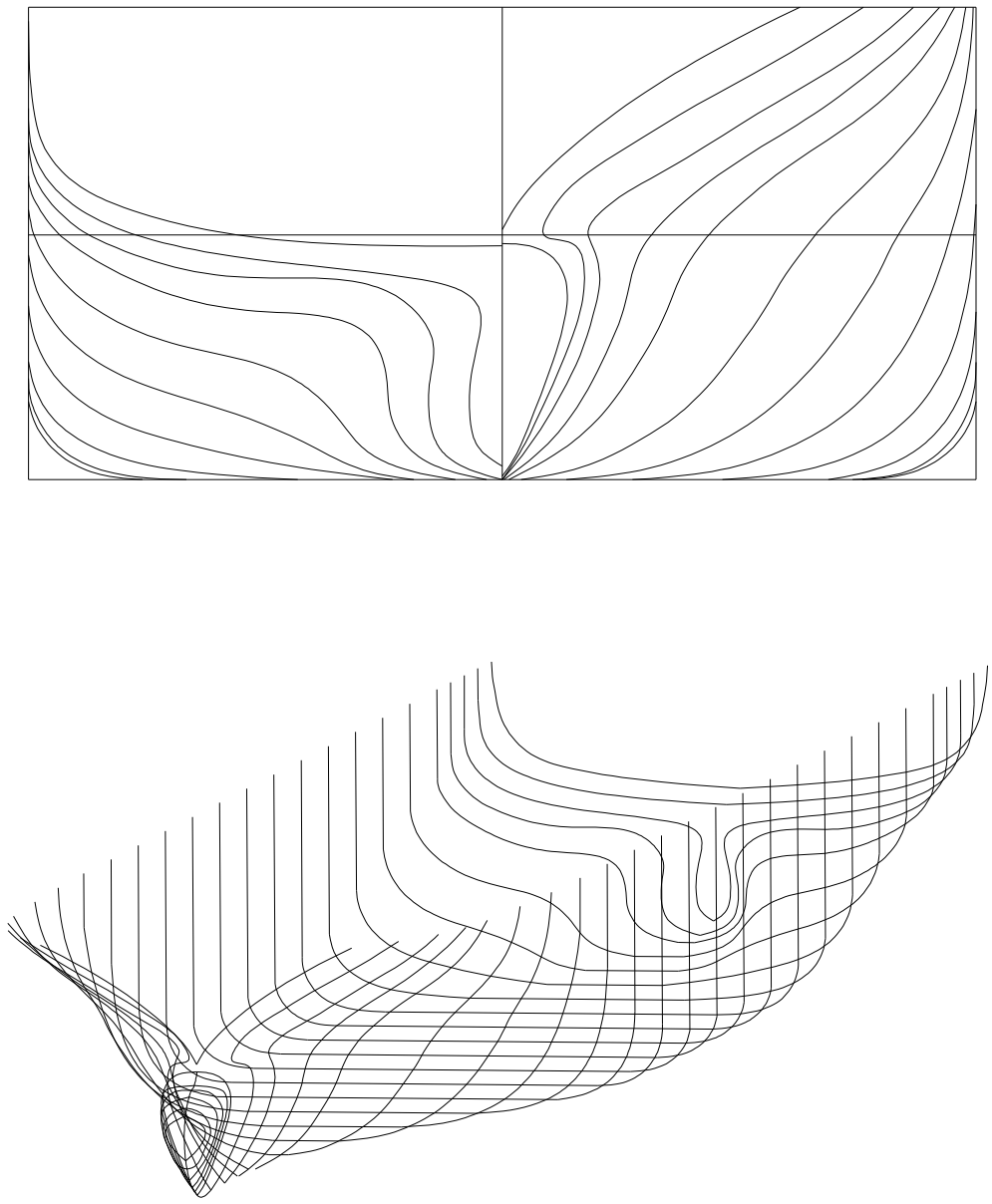

Fig 2.1 Hull form Designed

2.3 Hydrostatic Calculation

For the designed hull form, hydrostatic calculation is performed in view of the final dimension fixing.

Table 2.1 Hydrostatic Values for the Hull form Designed

DRAFT	DISPT	TPC	LCB	LCF	KB	TKM	LKM	MTC
[m]	[t]	[t/cm]	[m]	[m]	[m]	[m]	[m]	[t-m]
1.000	8753.48	96.45	0.61	0.22	0.52	139.83	5393.07	1272.33
1.500	13741.51	102.93	0.40	-0.17	0.79	101.33	3875.24	1435.06
2.000	19030.62	108.54	0.19	-0.54	1.05	82.13	3065.60	1571.97
3.000	30374.75	118.13	-0.23	-1.22	1.60	62.87	2202.08	1801.59
4.000	42612.43	126.52	-0.59	-1.69	2.15	53.17	1751.86	2009.70
6.000	69428.77	141.10	-1.00	-1.33	3.25	43.17	1287.20	2402.77
8.000	98791.38	152.39	-0.86	0.63	4.37	36.81	1057.95	2805.51
10.000	130370.12	162.84	0.01	4.52	5.50	32.76	943.35	3295.64
12.000	163677.28	169.97	1.17	7.09	6.62	30.02	832.53	3643.75
14.000	198345.80	179.26	2.62	13.81	7.73	28.53	788.09	4171.98
16.000	235230.81	189.85	4.90	19.98	8.87	27.95	773.17	4845.97
18.000	273881.47	196.41	6.99	19.05	10.02	27.33	731.09	5323.08
20.000	313685.75	201.51	8.35	16.35	11.16	26.88	686.55	5710.49
22.000	354431.00	205.84	9.10	13.43	12.29	26.67	644.97	6044.17
24.000	396012.06	210.02	9.39	10.26	13.42	26.66	611.72	6386.39
26.000	438385.41	213.67	9.33	7.38	14.54	26.80	581.24	6696.36
28.000	481458.84	217.02	9.04	4.96	15.65	27.12	553.32	6977.42
14.500	207359.25	181.78	3.13	15.41	8.02	28.31	781.59	4326.81

Table 2.2 Form Coefficients

DRAFT	CB	CP	CM	CW	AMS	AWP
[m]					[m^2]	[m^2]
0.500	0.3858	0.4971	0.7761	0.4144	21.81	8641.33
1.000	0.4096	0.5176	0.7914	0.4513	44.48	9409.71
1.500	0.4287	0.5319	0.8059	0.4816	67.94	10041.75
2.000	0.4452	0.5432	0.8196	0.5079	92.13	10589.75
3.000	0.4738	0.5605	0.8452	0.5527	142.50	11524.65
4.000	0.4985	0.5743	0.8680	0.5920	195.14	12343.59
6.000	0.5414	0.5985	0.9046	0.6602	305.04	13765.39
8.000	0.5778	0.6233	0.9271	0.7131	416.82	14867.36
10.000	0.6100	0.6481	0.9412	0.7620	528.98	15887.05
12.000	0.6382	0.6711	0.9510	0.7953	641.38	16581.96
14.000	0.6629	0.6920	0.9580	0.8388	753.78	17488.58
16.000	0.6879	0.7141	0.9633	0.8884	866.18	18522.40
18.000	0.7120	0.7360	0.9674	0.9190	978.58	19161.85
20.000	0.7339	0.7561	0.9706	0.9429	1090.99	19659.13
22.000	0.7538	0.7745	0.9733	0.9631	1203.42	20081.66
24.000	0.7721	0.7914	0.9756	0.9827	1315.87	20489.54
26.000	0.7889	0.8071	0.9775	0.9998	1428.35	20845.55
28.000	0.8046	0.8217	0.9792	1.0154	1540.84	21172.28
14.500	0.6691	0.6974	0.9595	0.8506	781.88	17735.11

Table 2.3 Main Dimensions

L_{BP}	371 m
B	56.2 m
D	28 m
T	14.5 m
C_B	0.669
C_M	0.9595
C_P	0.6974
C_W	0.8506

Chapter 3

Numerical Analysis using Ray Theory

3.1 Ray Theory

The bow waves of the ships are cancelled by the bulb waves so that the bow wave resistance is reduced considerably. Application of ray theory has found to have a profound implication in the field of bulb design by defining the pattern of waves being created in sea. Ray theory has been derived as an analogy to acoustics and optics. The approximate optimum size of the bulb is determined by minimizing the root mean square of the pressure differences near the bow between the excess of pressure on the mean surface caused by the double model hull and by the bulb.

Consider the ship that advances with a constant velocity U on the free surfaces and produces waves. A rectangular coordinate system is attached to the ship bow at the mean surface with the x-axis in the direction of U and the z-axis directed positive upward; the flow field is considered relative to the ship. The Ray is defined as the path of the wave energy packet carried downstream. If the sip has a smooth hull, the ship waves for a slow ship may be divided into two systems or sources of waves: bow and stern waves. Thus only two systems of waves can only be considered as far as the full ship wave system is to be considered: bow and stern ray systems. The wave energy that propagates in the resultant direction of the vector sum of the flow velocity and group velocity.

The ray theory has been applied in designing and assessing the wave pattern around the ship and to check the generation of caustics. Ray theory is evaluated here as an extension of

linear wave theory. In linear theory, the wave propagation on a calm water surface, the dispersion relation [2] & [7] is given by

$$\omega^2 = gk \tag{1}$$

where ω is the wave frequency. When ship with a constant velocity U is considered, the wave field must be steady relative to the ship. Therefore, the wave speed in the direction normal to the wave crest is $c = \frac{\omega}{k} = U\cos\theta$, from which,

$$\omega = kU\cos\theta = kc \tag{2}$$

Therefore, $$k = \frac{g}{U^2\cos^2\theta}$$

3.1.1 Assumptions of Ray theory

1. The Ray equation is independent of k_o and Froude number F_N, because k_o is a constant multiplier of the wave number in non-uniform flow and cannot influence the irrotationality of the wave number vector.
2. Ray path is independent of Froude Number
3. Ray paths follow a straight line despite of the ambiguity at the stagnation point

3.1.2 Mechanism of Bulb Waves

In general, the major bulb waves are elementary sine waves with the origin at the bow. Ideal bulbs produce negative sine wave having a phase exactly opposite to that of the bow waves. The amplitude of any bow wave is a function of Θ, and the bulb wave amplitude can be matched up with the ship bow wave amplitude by a distribution of doublet strength along the

stem line at the bow. In fact, in the ideal situation, the total bow wave can be completely nullified by a proper distribution of the doublet strength along the negative z-axis. The doublet distribution is a function of Froude number and becomes larger as the Froude number increases. And when the Froude number is small, the wave length is reduced and the linear wave resistance is small.

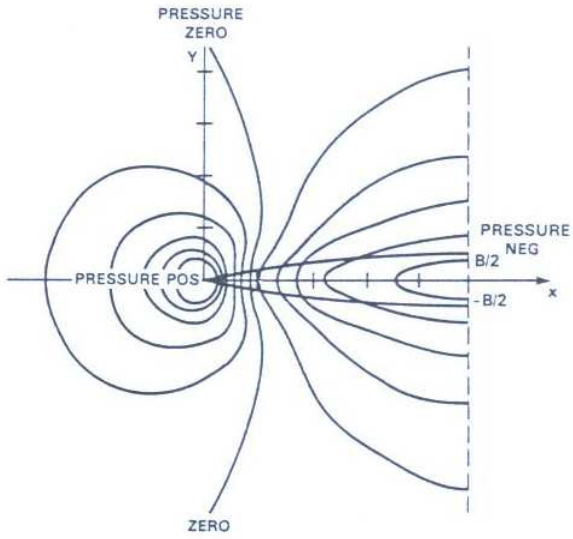

Figure: 3.1 Pressure Distributions around the Bulb

Near the ship, the wave slopes become large and the wave break not only because the flow near the bow is strongly perturbed, but also the rays at small values of Θ intersect each other after reflection. This is a non linear phenomenon and ray theory can predict the formation and approximate location of the caustics where the wave breaking occurs. If the flow field is superimposed and a proper size of the bulb is used, the region near the bulb the excess pressure caused by double model is largely cancelled by the bulb's opposite pressure. In addition, the ray paths of the bulbous ship indicate that the bulb decreases the non-uniformity of the flow

3.2 Derivation of Ray Equation

The ray equation for analysis is derived from the killer's dispersion relation for a non-uniform flow field. The ray equation is obtained form the irrotationality of wave number vectors [2].

$$\nabla \times k = \nabla \times \nabla s = 0 \tag{3}$$

The velocity vectors both along the x direction and y directions are termed as u and v. According to ray theory, the equations for the velocity vectors are formulated as follows.

$$\frac{dx}{dt} = 2\sin\theta(u\sin\theta - v\cos\theta) + (u\cos\theta + v\sin\theta) \tag{4}$$

$$\frac{dy}{dt} = -2\cos\theta(u\sin\theta - v\cos\theta) + \sin\theta(u\cos\theta + v\sin\theta) \tag{5}$$

The waterline for the double model ship on the plane of symmetry at the mean surface is obtained from

$$\frac{dx}{dt} = u \quad \& \quad \frac{dy}{dt} = v \tag{6}$$

3.2.1 Rays of Bulbous Ships

In ray theory, a ray is represented by a point doublet source strength μ is given by an approximate relationship with bulb radius [7]

$$\frac{\mu}{UL^3} = 0.5\frac{r_b}{L^3} \tag{7}$$

Where r_b is the bulb radius and L is the length of the load waterline of the ship. Using the velocity equations ray paths are computed for different bulb sizes and different entrance angles. A bow bulb is represented by a simple point doublet whose direction is along the negative axis. The potential is positioned at (0, 0, d), where d is the depth of draft line for different speeds. If

a double model potential is considered, the image doublet at (0, 0, d) with the same strength has to be considered and the total potential on the mean surface is $2\Phi_d$. Thus the velocity components at (x, y, 0), which will be used for the ray equations are as follows:

$$u = -2\mu(\frac{1}{r^3} - \frac{3x^2}{r^5}) \tag{8}$$

$$v = 6\mu\frac{xy}{r^5} \tag{9}$$

3.3 Solution of Ray Equations for Computing the Ray Paths

Ray Equation is solved assuming that the wave number is constant along the ray path and the different rays emanated can only be assessed by large angle variation because of the ambiguity near the stagnation point where all the Ray equations tend to collapse.

Comparing the equations (3)-(7),

$$u = 2\sin\theta(u\sin\theta - v\cos\theta) + (u\cos\theta + v\sin\theta)\cos\theta$$

I.e. $u = 2u\sin^2\theta - 2v\sin\theta\cos\theta + u\cos^2\theta + v\sin\theta\cos\theta$

Ie $u(2\sin^2\theta - 1 + \cos^2\theta) + v(\sin\theta\cos\theta - 2\sin\theta\cos\theta) = 0$

Ie $u\sin^2\theta = v\sin\theta\cos\theta$

Or $\tan\theta$ = v/u

Similarly, for the velocity v,

$$v = -2\cos\theta(u\sin\theta - v\cos\theta) + \sin\theta(u\cos\theta + v\sin\theta)$$

I.e. $v = -2u\cos\theta\sin\theta + 2v\cos^2\theta + u\sin\theta\cos\theta + v\sin^2\theta$

I.e. $u(-2\cos\theta\sin\theta + \sin\theta\cos\theta) + v(\sin^2\theta + 2\cos^2\theta - 1) = 0$

I.e. $v\cos^2\theta = u\sin\theta\cos\theta$

Or $\tan\theta$ = v/u

The above two solutions shows that the equations are consistent and tend to have a unique solution. Hence, it is enough to apply one of the two equations for plotting the ray paths.

From equations (8) and (9)

$$\frac{v}{u} = \tan\theta = \frac{6\mu \frac{xy}{r^5}}{-2\mu\left(\frac{1}{r^3} - \frac{3x^2}{r^5}\right)}, \tag{10}$$

Where x and y represents the coordinates of the water plane under consideration. Solving the above equation,

$$\tan\theta = \frac{-3xy}{r^2 - 3x^2} \tag{11}$$

3.4 Optimum Bulb Radius

Bulb parameters can be derived by the concept of Double body potential with linear wave theory in a close compromise with Ray Theory. The matching up of an amplitude function of a doublet, which is a function of the doublet strength and the Froude number, is taken into account for the computation. With an optimum doublet distribution at the bow and stern, the waves from bow and stern of the given symmetric ship may be completely cancelled and in theory, ideal fluid resistance of the ship become zero. In this analysis, an in viscid, incompressible and homogenous fluid in steady flow with a free surface and of an infinite depth is considered. The coordinate system O-xyz is right handed with the origin on the mean surface, x positive in the direction of the uniform flow velocity V, and z positive in the upward direction. The analysis has been performed by non-dimensionalizing the x and y coordinates

with respect to L; z is non-dimensionalized with respect to draft H, and m is non-dimensionalized with respect to V and LH. All wave heights components are considered to small and additive.

It is well known that a point source of strength m located at a point (x_1, 0, z_1), where $z_1>0$, produces a wave height non-dimensionalizd with respect to L at large x given by (Havelock, 1951[5]),

$$\varsigma_S = 8k_0 \int_0^{\pi/2} me^{-k_0 z_1 \sec^2\theta} \sec^3\theta \cos[k_1(x-x_1)\sec\theta]\cos(k_1 y \sin\theta \sec^2\theta) d\theta \tag{12}$$

where $k_1 = \frac{Lg}{V^2}$ and $k_0 = \frac{Hg}{V^2}$

A Simple Source and a Doublet in a Uniform Stream is assumed to be placed in the ship's bow at the free surface with origin at (0, 0, d) where d represent the draft for the ship. Let the point doublet with the strength $\mu>0$ at complex potential surface with z = x + iy = 0 combined with a strength m>0 at $z = z_0$. Then the complex potential W will be written as

$$W = -Vz - m\log(z - z_0) + \frac{\mu}{z} \tag{13}$$

The complex potential can be split as $W = \phi + i\psi$ where ϕ, real part represents the Potential function and Ψ, imaginary part of the complex potential represents the steam function.

To separate the stream function,

$$W = -V(x+iy) - m\log\{(x+iy) - (x_0 + iy_0)\} + \frac{\mu}{x+iy}$$

Hence, the steam function is

$$\psi = -Vy - m\tan^{-1}\frac{y-y_0}{x-x_0} - \frac{\mu y}{x^2+y^2} \tag{14}$$

Where V is the velocity in the Y direction, m is the strength of source and x & y represents the coordinates of the surface under consideration.

In polar coordinates,

$$x = r\cos\theta; y = r\sin\theta$$

Where r represent the coordinate radius from the origin and θ represent the angle subtended by the radius r with respect to the origin.

Hence, $\psi = -Vr\sin\theta - m\theta_1 - \frac{\mu\sin\theta}{r}$

Where $\theta_1 = \tan^{-1}\frac{y-y_0}{x-x_0}$

Hence the body streamlines is obtained by putting $\psi = -m\pi$. Non-dimensionalizing the equation (14) by $Vh = m\pi$, finally the equation takes the from;

$$R^2\sin\theta + R\frac{\theta_1}{\pi-1} + \mu_1\sin\theta = 0 \tag{15}$$

where $R = \frac{r}{h}$ and $\mu_1 = \frac{\mu}{Vh^2}$.

The streamline due to a source in the uniform flow is well known from Milne Thomson 1955 equation. The combination of source and a positive doublet will produce a neck and hence the strength of the doublet should satisfy $\mu_1 = \frac{\mu}{Vh^2} < \frac{1}{4}$ for all streamlines.

3.5 Ray Theory Computational Results

For the different bulb shapes derived, the ray equations derived are used to calculate the ray paths and plotted at the free surface height and the results are shown in figs (3.3) to (3.8). The entrance angle for the different shapes are also estimated form the plot and it's evident that the creation of secondary waves called caustics in Ray theory in some sections are not desirable. Hence, ray theory provides a strong view point to isolate the sections which are ideal for the hull form under design.

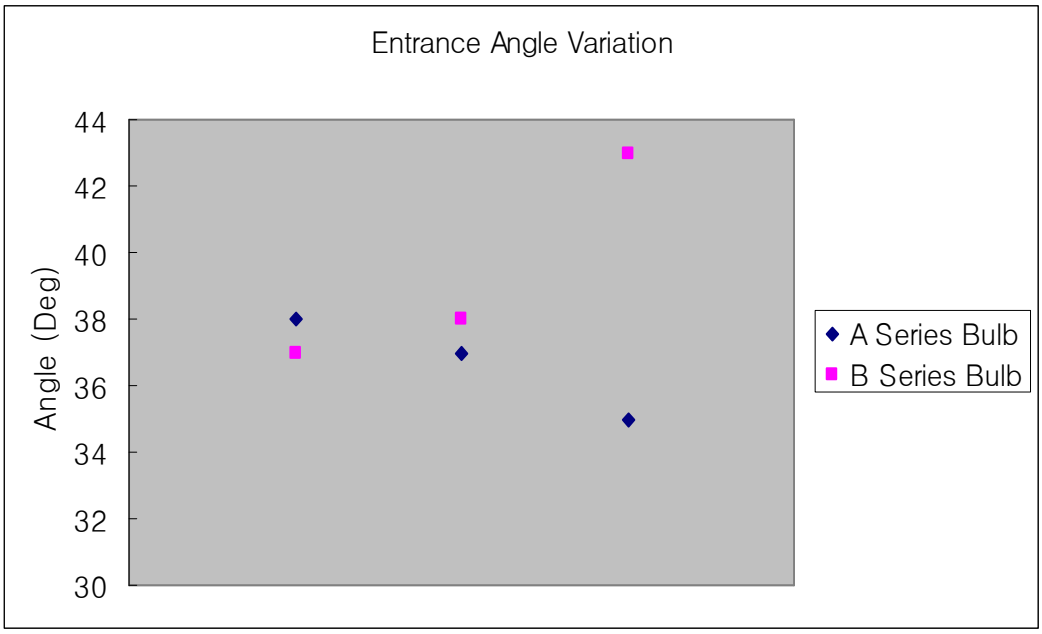

Fig 3.2 Entrance Angle Variation

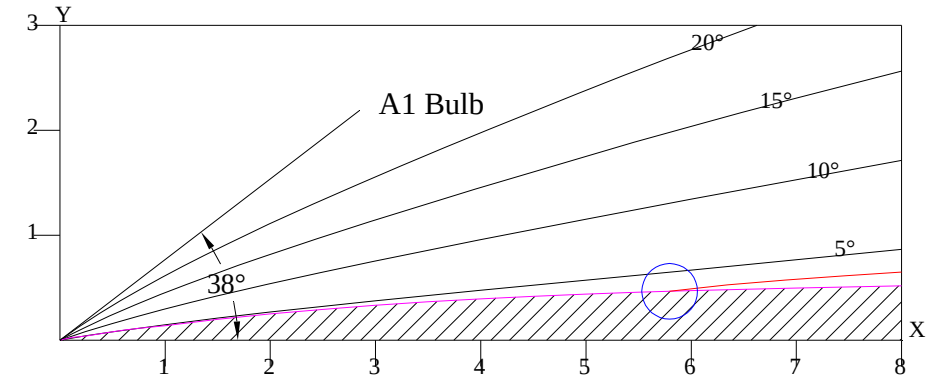

Fig 3.3 Ray Paths for A1 Bulb

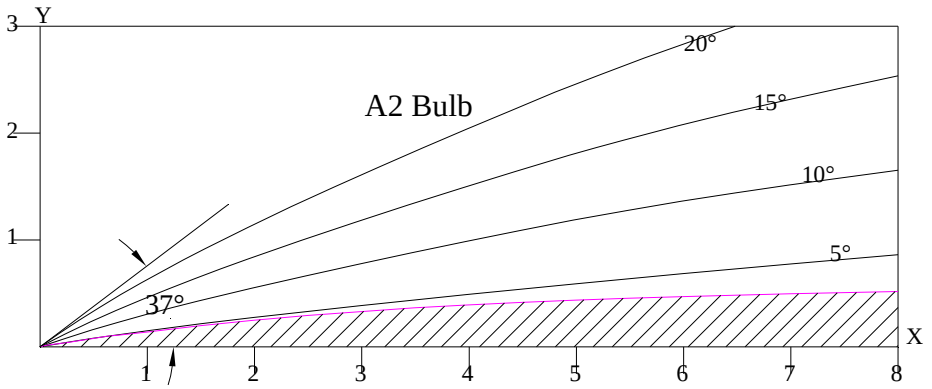

Fig 3.4 Ray Paths for A2 Bulb

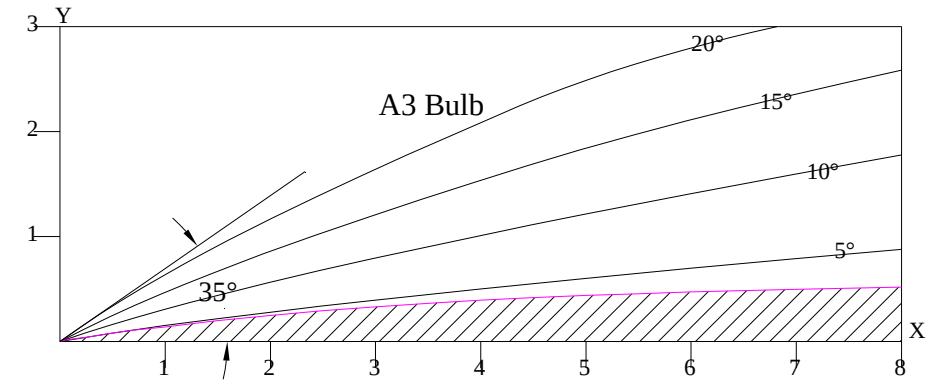

Fig 3.5 Ray Paths for A3 Bulb

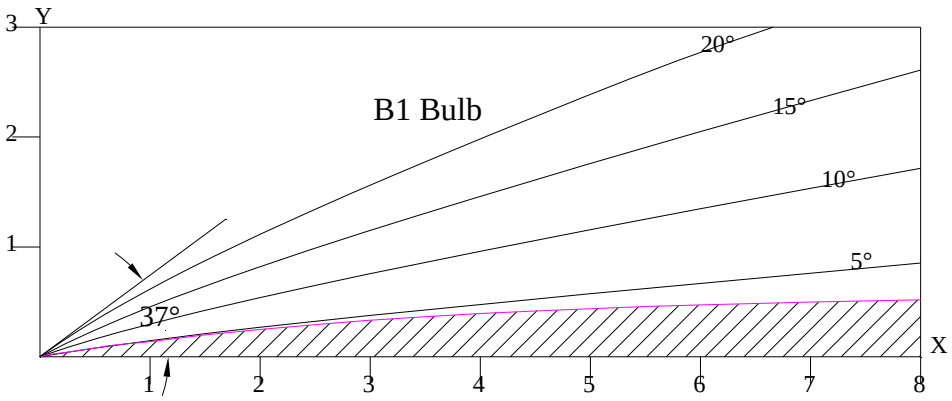

Fig 3.6 Ray Paths for B1 Bulb

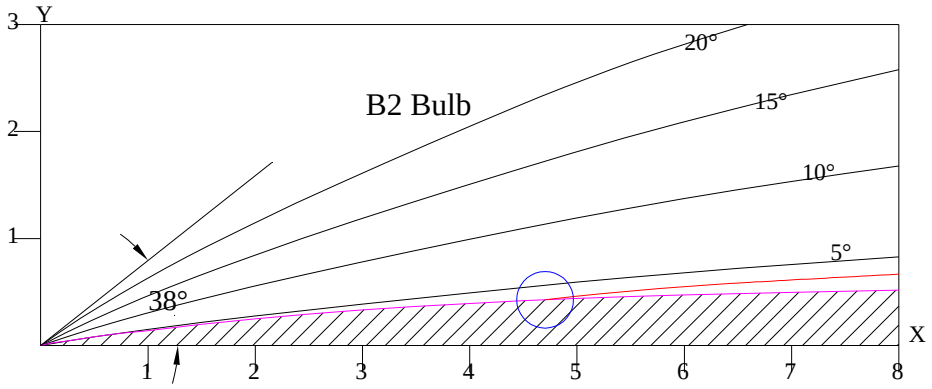

Fig 3.7 Ray Paths for B2 Bulb

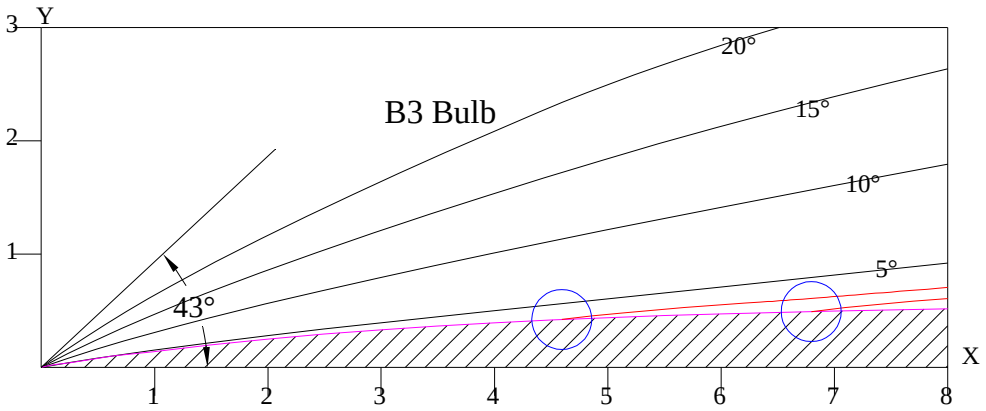

Fig 3.8 Ray Paths for B3 Bulb

Wave Height Calculation and 3 D Interpretation of Bow Wave

The Steady Surface wave [13] pattern z = $\varsigma(x, y)$ of any moving body is of the form of a sum of plane waves traveling at various angles of propogation relative to the direction of motion of the body.

$$\varsigma(x, y) = \int_{-\pi/2}^{\pi/2} A(\theta) e^{-i\Omega(\theta)} d\theta \tag{16}$$

Where, $\Omega(\theta) = k(\theta)[xCos\theta + ySin\theta]$ is a phase function. Here A (θ) is the amplitude and *k (θ)* is the wave number of the wave component traveling at angle θ. For the further analysis of the 2 Dimensional calculations of the Ray paths, the depth factor in the z-axis is taken into consideration. For the computation of wave amplitude, the double integral over the body's centre plane, determining *A*(*Θ*) for each fixed angle from the offsets *Y*(*x; z*), can be reduced to a pair of separate integrals over depth and length as follows.

First evaluate for all stations *x* the integral

$F(x, \theta) = \int Y(x, z) e^{kzSec^2\theta} dz$ and integrated in the vertical z direction. As for the bulb case study, the fore most part of the hull is concentrated with in a small control volume with an incoming flow velocity U. With respect to the change in bulb volume, each change in bow wave height is calculated assessed. The wave amplitude A(*Θ*) is given by the equation,

$$A(\theta) = -\frac{2i}{\pi} k^2 Sec^4\theta \iint Y(x, z) \exp(kzSec^2\theta + ikxSec\theta) dxdz \tag{17}$$

For further integration of the equations, Mathematica 4.1 software is used.

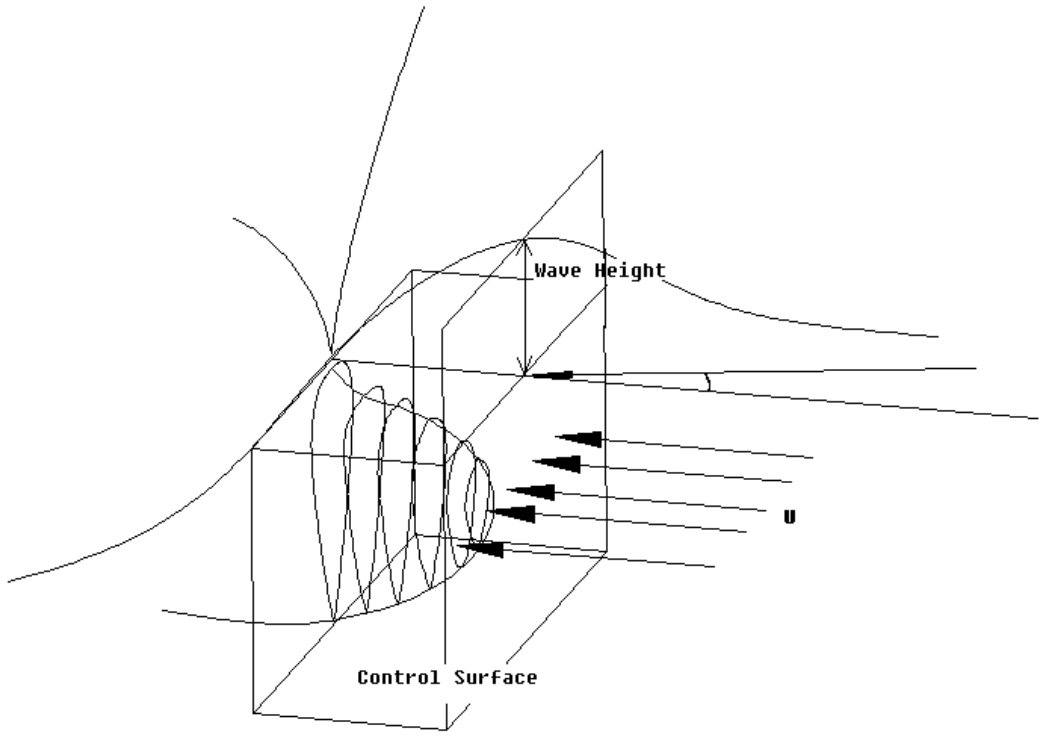

Fig 3.9 Control Surface surrounding the Bulb

$k = \frac{g}{U^2}$ = 0.030705

The Ray equation calculated in Fig 3.3 to 3.8 has been integrated along the z direction of the ship profile with limits from 0 to draft height.

Ray Wave =

$$\text{Sec}[\theta]\text{^}4 \int\int \left(\frac{0.0114\,x\,y}{-0.0466 + 0.0114\,x^2} \right) \text{Exp}[0.03075\,z\,\text{Sec}[\theta]\text{^}2]\,dx\,dz$$

Table 3.1 Wave Height at F.P for 'A' and 'B' Series Bulbs

Bulb	Wave Height/L_{PP} at F.P
A1	0.0256
A2	0.0243
A3	0.0238
B1	0.0288
B2	0.0248
B3	0.0252

The Amplitude function A(Θ) has a direct relation to the wave making resistance and it is interpreted as the total energy left behind in the wave field and it is given by the Michelle's integral for wave resistance.

$$R = \frac{\pi}{2}\rho U^2 \int_{-\pi/2}^{\pi/2} \left|A(\theta)\right|^2 Cos^3\theta d\theta \qquad (18)$$

where ρ is the density, U is the speed and Θ is the Entrance angle. The thin-ship theory of Michelle represents the body by a centre plane source distribution proportional to its longitudinal rate of change of thickness (local beam). The only requirement for its validity is that that quantity be small. Hence the theory applies as well to submerged as surface-piercing bodies. In some cases especially for submerged bodies it is possible instead of thin-ship theory to use the somewhat simpler "slender-body theory", where the body is represented by a line of sources rather than a plane distribution, but we shall not use slender body theory in the present

report. In any case, the thin-ship theory includes the slender-body theory, and specifically gives the latter as a limit of the former for large beam/draft ratios. In general, there is no restriction on beam/draft ratio for validity of thin-ship theory, so long as the beam/length ratio is small.

CHAPTER 4

THE KRACHT BULB DESIGN

A body that moves on the undisturbed surface of the water produces a wave system. This system is generated by the field of pressure around the body and the energy possessed by the waves is given to them by the body itself. This transfer of energy from the body to the surrounding system generates a directional force opposite to that of the movement, which is the wave resistance.

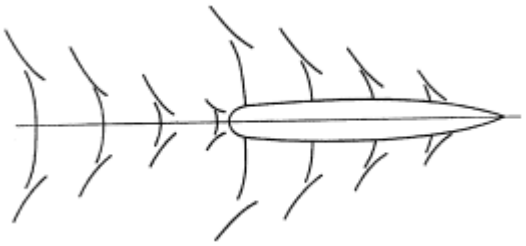

Fig: 4.1 Schematic diagram of the wave system generated by the bow and the stern

There are two kinds of wave systems generated by ships, diverging ones that form laterally to the ship that have inclined crests with respect to the ship's symmetrical level and transversal ones that form at the bulwarks of the ship that have perpendicular crests with respect to the centerline (see Figs. 4.1 and 4.2). This wave system, divergent and transversal, is generated by both the stern and the bows. The interference between these waves systems creates the characteristics ups and downs based on speed-length ratio $V/\sqrt{Lwl}$ in the wave resistance curve. Considering only the transversal waves, in a simplistic but indicative way, it can be said that wave resistance is given by the difference between the pressures at the bow area, in the

direction bow-stern, and the pressures at the stern area in the direction stern-bow. While the bow-stern pressure system increases constantly with the increase in $V/\sqrt{Lwl}$, the stern-bow pressure system is variable (in other words it can be positive or negative) depending on the interference between the waves systems at bows and stern. There will therefore be a crest in the wave resistance when there is a (wave) trough at stern and vice versa a trough in the wave resistance when there is a (wave) crest at the stern. Based on the above, ship's wave resistance depends on the speed, length and shape of the bottom, in other words on the penetration angle of the water lines and the distribution of volume in a longitudinal, transversal and vertical direction.

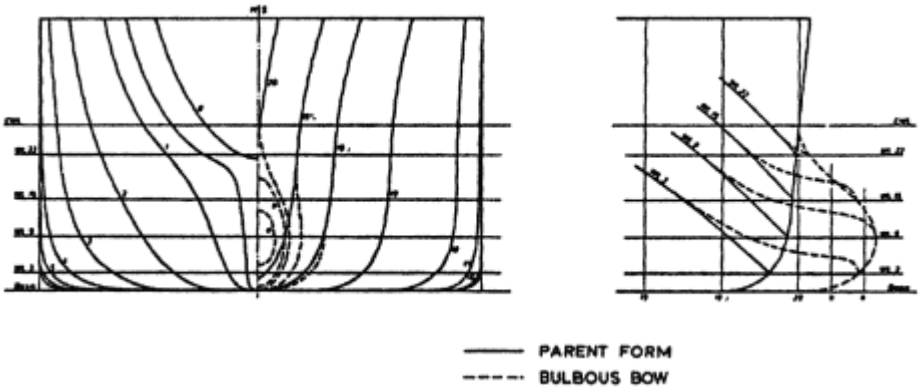

Fig: 4.2 The bulbous bow as it modifies the penetration angles and volume distribution represents an effective means for reducing wave resistance

Hence the bulbous bow’s own wave system interferes with the ship's wave system. The longitudinal position of the bulbous bow defines the interference phase, while its volume determines the width of its wave system.

A certain shape of bulbous bottom is excellent only in design conditions. Usually at low speeds the effect of the bulbous bottom is negative, while as the Froude number (Fn) increases it becomes positive and increases up to a maximum value, from this point on, for Fn, which tends to the infinite, the bulbous effect tends to zero.

Thus the decision for or against the adoption of a bulbous bow depends on an analysis of costs and benefits. However, it can be affirmed that the good hydrodynamic shape of a bottom with moderate wave formation does not usually need a bulbous bow, while this is necessary in the presence of a considerable wave formation due to the poor "starting" of the bottom shapes. Obviously "starting" does not mean geometrically but hydro-dynamically. In fact if geometric starting were sufficient, a computer with starting programs for bottoms would have resolved all the problems. But unfortunately good hydrodynamic start up depends on the skill and experience of the designer and the specialist in naval architecture (a subject that includes the study of boat static and the dynamics).

In fact the starting of shapes creates pressure and depression components that act on the bottom and which generate a rise or lowering in the water level, when the value of the pressure undergoes a positive or negative variation. The water lines that define the bulb towards the prow must have a well started hydrodynamic profile, to avoid separation of the fluid filaments. The upper part of the bulb must be connected with the body of the ship well so that the water, flowing over the body of the bulb itself, can interfere favorably with the residual bow wave. For each bulbous bottom, there is an optimal condition, corresponding to a speed that can be

determined experimentally. From all this it is evident that the influence of the bulb must not be considered limited to the bow wave formation, but that it extends to the so-called separation or shape resistance, that is the viscous type resistance that, together with wave resistance, is referred to in the term residual resistance, including pressure viscous resistance, resistance due to vortexes, cavitation, etc.

Moreover, an opportunely started bulb, due to its high damping characteristics, considerably reduces the bow acceleration due to pitching and therefore has a positive effect on sea keeping. Optimum choice of a round bottom depends on the skill of the designer in achieving the best compromise between weight, volume and speed. As always the designer's ability is fundamental, from whose skill in realizing the best compromise between weight, volume and speed creates the optimum choice of a round bottom.

4.1 Bulb Shape for Container Ships

Unlike any other cargo carriers, container ships demand speed and safety in transport. Hence an ideal high speed bulb has to be fitted in compromising fashion with the hull form designed. High speed inverted bulb shapes are generally preferred for container ships with excellent performance both form resistance and sea keeping point of view.

The main bulb parameters that affect the bulb design and overall ship performance are listed below:

Bulb Cross sectional Parameter C_{ABT}

Bulb Nose Height Parameter C_{ZB}

Bulb Breadth	Parameter	C_{BB}
Bulb Length Parameter		C_{LPR}
Bulb Lateral Parameter		C_{ABL}
Volumetric Parameter		C_{VPR}
Froude Number		F_N

For an adequate presentation of the hydrodynamic properties of bulbs, it is necessary to systematize the different existing forms and the various characteristics of the bulb associated with it. For the current design, the Nabla type inverted drop shaped bulb is decided owing to its overall high speed performance. The nabla bulb has centre of area situated in the upper half part, indicating a volume concentration near the free surface.

With respect to the lateral contour of the bulbous bow, two typical classes are distinguishable:

1) The stem outline remain unchanged as with Taylor concept design of bulb
2) The stem outline is changed by the protruding bulb as with all modern bulbous bows.

4.2 Bulb Parameter Definitions

1. The breadth parameter, that is, the maximum breadth B_B of bulb area A_{BT} at the F.P divided by the beam B_{MS} of the ship

$$C_{BB} = B_B/B_{MS}$$

2. The length parameter, that is, the protruding length L_{PR} normalized by the L_{PP} of the ship

$$C_{LPR} = L_{PR}/L_{PP}$$

3. The depth parameter, that is, the height Z_B of the foremost point of the bulb over the base divided by the draft T_{FP} at the F.P

$$C_{ZB} = Z_B/T_{FP}$$

4. The cross-sectional parameter, that is, the cross-sectional area A_{BT} of the bulbous bow at the F.P divided by midship sectional area A_{MS} of the ship

$$C_{ABT} = A_{BT}/A_{MS}$$

5. The lateral parameter, that is, the area of the bow profile in the longitudinal plane normalized by A_{MS}.

$$C_{ABL} = A_{BL}/A_{MS}$$

4.3 Analysis Method

As the definition of an optimum bulb shape includes innumerable number of parameters to be dealt with, it is required to conclude on vital properties to delineate and to design the bulb. The two main parameters that affect the bulb properties and hence the overall ship resistance are the bulb cross section shape or area and the node height with respect to the free surface. As the ship varies the trimming angle at different speed, both the parameters keep on changing and hence an optimum design unravels the investigation of these two parameters in the overall performance of the bulb.

According to Alfred M Kracht (1978) [1] design methodology, different shapes of the bulbs are designed and incorporated into the designed hull form for the ULCS.

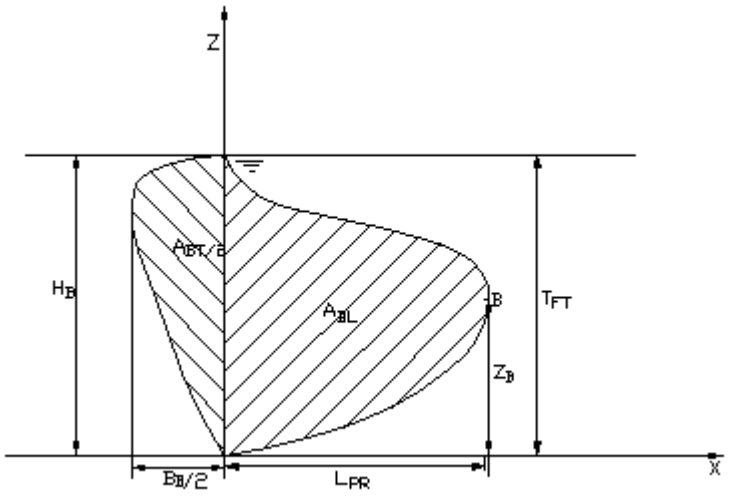

Fig: 4.3 Linear and Non-Linear Bulb Quantities

Two different series of bulbs are analyzed depending up on the variation of cross sectional parameter and the nose height and the respective series are termed as A Series and B series and the performance of each bulb is compared with a bulbless hull form for the same ship keeping the block coefficient same.

From the main dimensions calculated, to calculate the bulb parameters and power reduction calculation due to the bulb effect is done with design charts for corresponding block coefficients. For this, L_{BP}, B_{MS}, T_{MS} and Fn are considered. The bulb parameters depending on the ship's main dimensions are delineated as shown below.

Table 4.1 'A' Series (C_{ABT} Varied)

	C_{VPR}	C_{ZB}	C_{ABT}	C_{ABL}	C_{LPR}	C_{BB}
Min	0.221	0.6	0.09	0.12	0.028	0.145
Avg	0.315	0.6	0.115	0.141	0.034	0.15
Max	0.381	0.6	0.132	0.155	0.038	0.171

Table 4.2 'B' Series (C_{ZB} Varied)

	C_{VPR}	C_{ZB}	C_{ABT}	C_{ABL}	C_{LPR}	C_{BB}
Min	0.221	0.7	0.09	0.12	0.028	0.145
Avg	0.315	0.85	0.09	0.141	0.034	0.15
Max	0.381	0.96	0.09	0.155	0.038	0.171

4.4 Bulb Sections

The hull form designed previously has been faired with various bulb shapes as prescribed above in AutoCAD keeping the volume and LCB same as far as possible. The bulb parameters are taken into consideration in the design as per Tables 4.1 & 4.2.

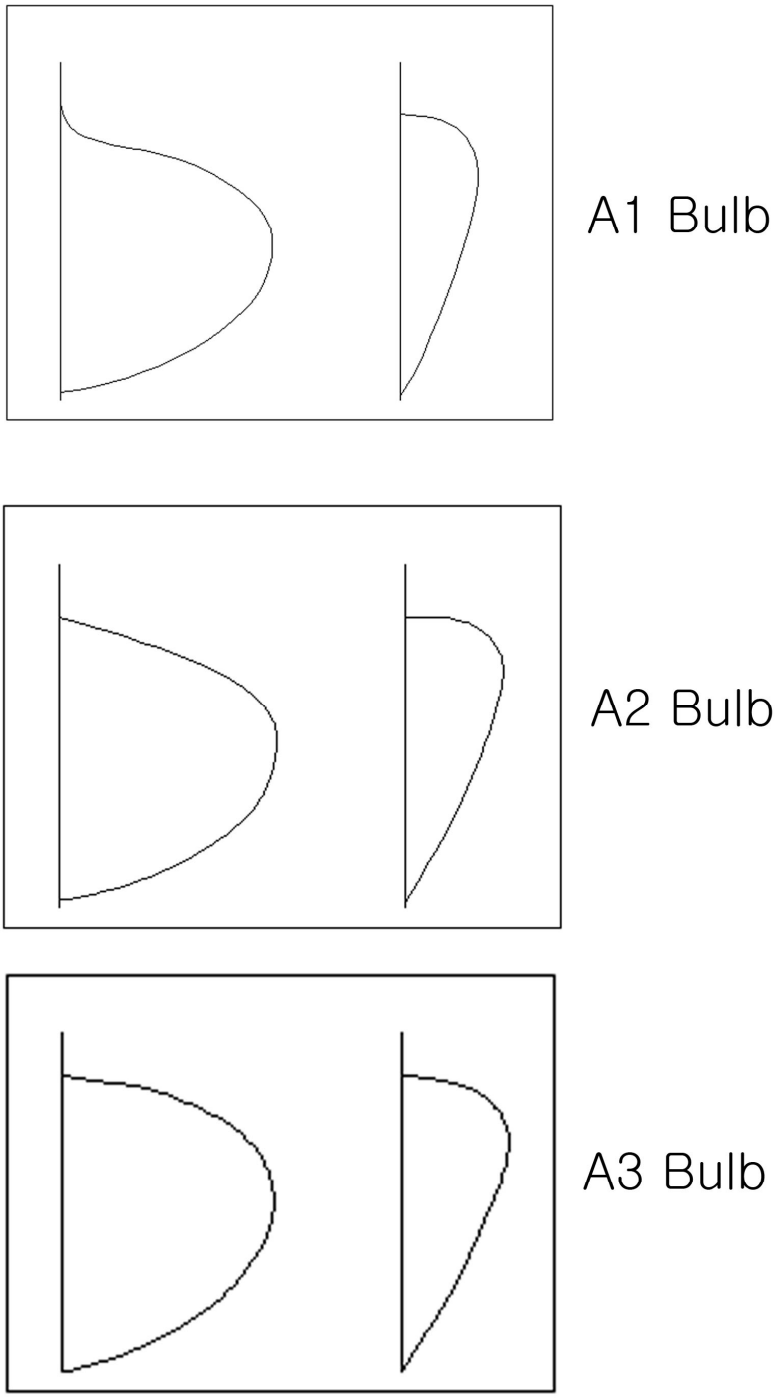

Fig 4.4 A Series Bulb Sections

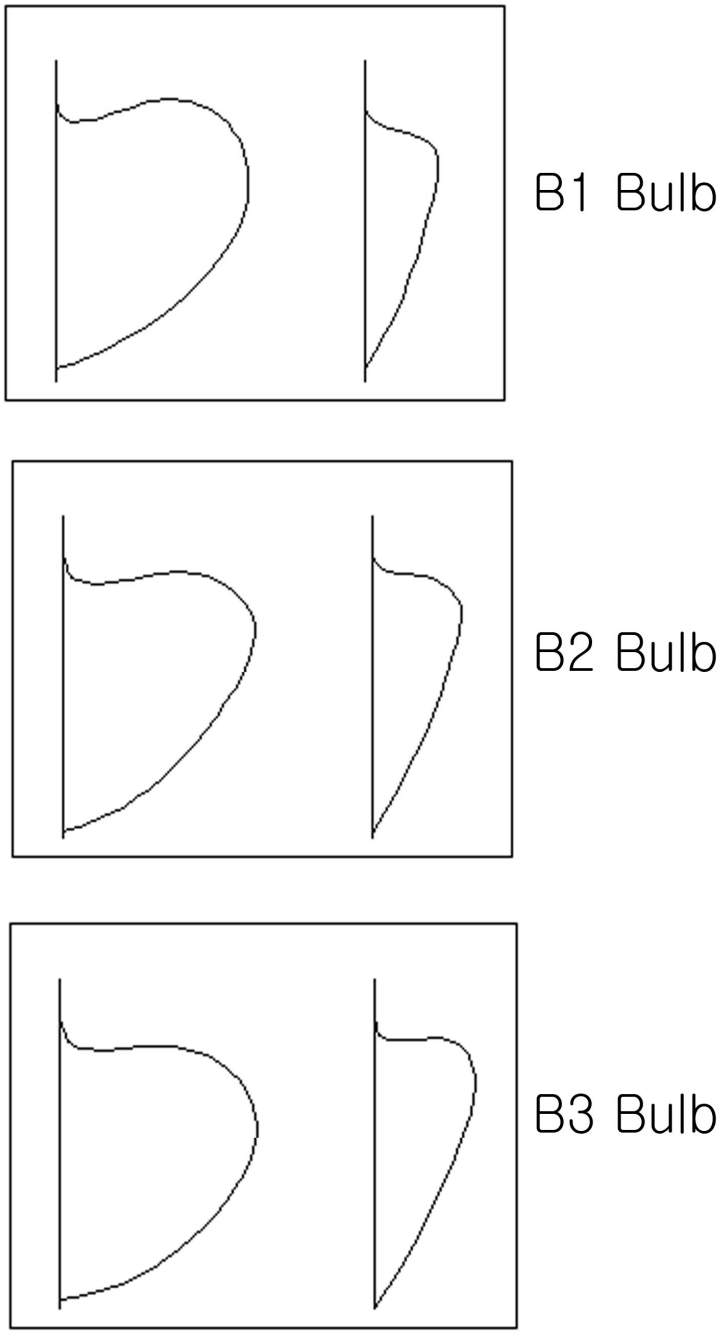

Fig 4.5 B Series Bulb Sections

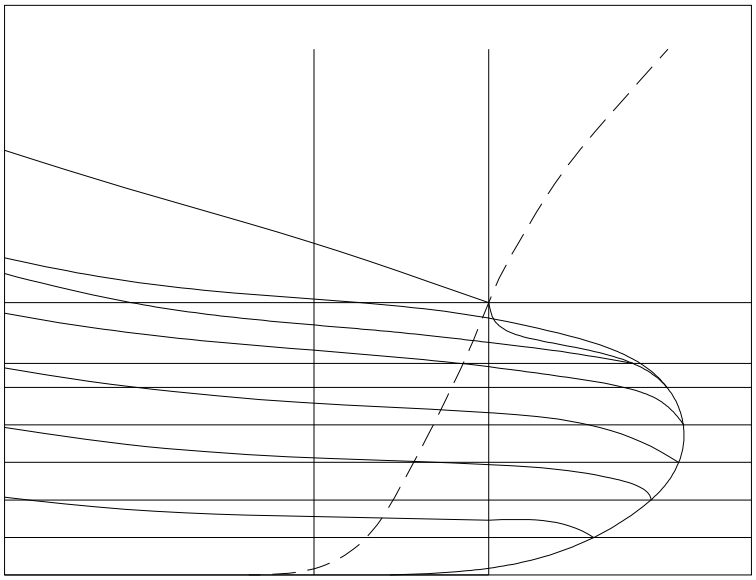

Fig: 4.6 Bulb Variation in comparison with Bulbless Bow

4.5 Power Reduction Method by Kracht Theory

4.5.1 Influence of Bulbous Bow on the Properties of the Ship

The effect of bulb on resistance in turn influences the ship's overall performance and propeller loading calculations. The propulsive characteristics of the shi such as Quasi-Propulsive coefficient, the wake and the thrust deduction factor have a remarkable change with the change in design of bulb for a particular hull form. All these factors are compared with respect to a bulbless hull form. Figs 4.6 will give an idea about the influence of bulb in thrust reduction, axial wake distribution and wake fraction.

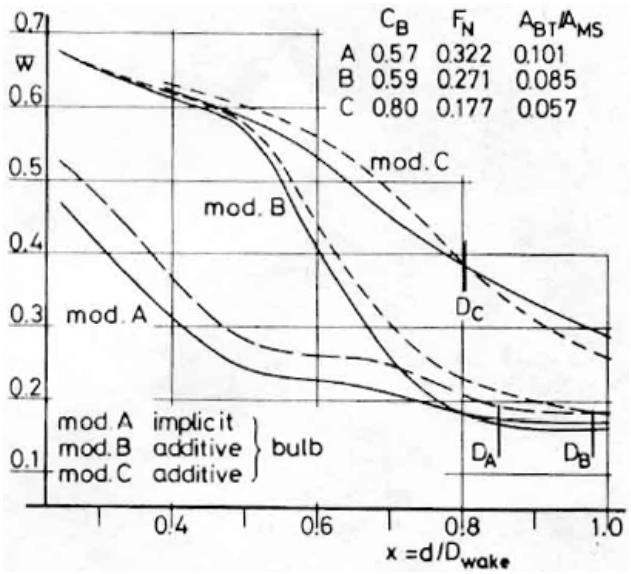

Fig: 4.7 Influence of Bulbous Bow on Nominal Axial Wake

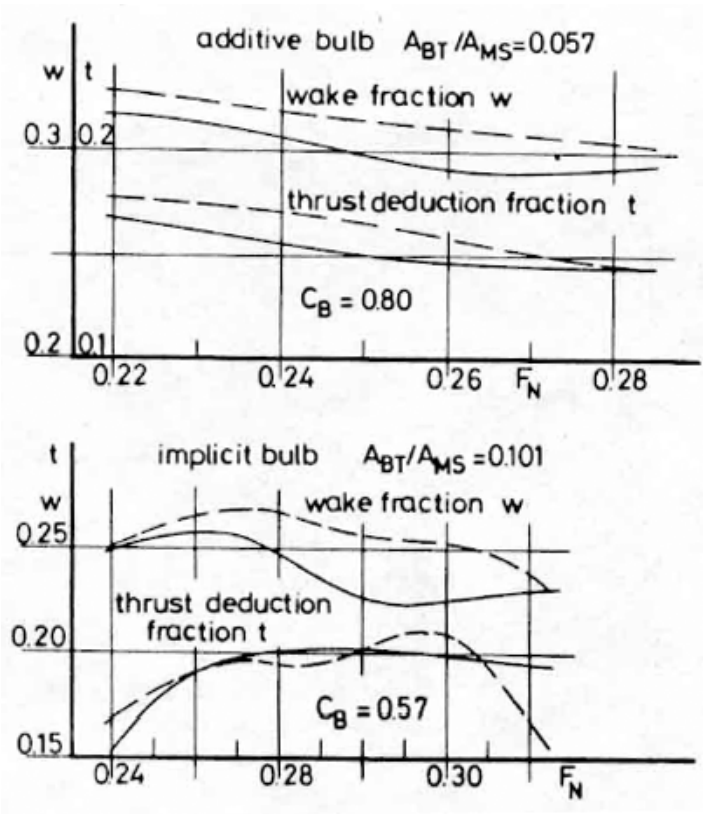

Fig: 4.8 Influence of Bulbous Bow on Thrust Reduction and Wake Fraction

The most important effect of a bulbous bow is its influence on the different resistant components and the total power output. Kracht design methodology follow a systematic sequence of division of resistance components as formulated below:

$$R_T = R_V + R_{WF} + R_{WB} = R_F + R_{VR} + R_{WF} + R_{WB}$$

Where

R_V = Viscous Resistance

R_F = Frictional Resistance

R_{VR} = Viscous Residual Resistance

R_{WF} = Wave-making Resistance

R_{WB} = Wave-breaking Resistance

The later two components are related to wave making resistance and their contributions to the total resistance are vital. The additional bulb surface area always increases the bulb resistance R_F. According to this theory, bulb is a pure interference problem of the free wave systems of the ship and the bulb. Depending on the phase difference and the amplitude, a total mutual cancellation of both interfering wave systems occur. The position of the bulb body causes the phase difference, while its volume is related to the amplitude. The wave resistance analysis is based on the free wave pattern measured in the model experiments.

The wave breaking resistance R_{WB} depends directly on the rising and development of the free as well as the local waves in the vicinity of the fore body and understanding the wave breaking phenomenon of the ship waves is important for the bulb design for the full ship.

4.5.2 Bulb Effect

At constant Froude number Fn, the bulb effect is a function of all six bulb parameters:

$$\Delta R = F(C_{VPR}, C_{ABT}, C_{ABL}, C_{LPR}, C_{BB}, C_{ZB})$$

This multi dimensional relationship complicates the understanding of the dependencies on single parameters. According to the linearized theory, the interference effect depends on the volumetric parameter C_{VPR} in a quadratic manner. It is a measure of amplitude of wave pattern. The breaking effect also shows a similar breaking effect.

For a constant bulb volume and depth, the length parameter C_{LPR} has a great influence on the interference effect. As it is a measure for the phase relation of the free wave systems of ship and bulb, typical maxima and minima appear as a direct consequence of interference waves.

The dependence of the interference effect on the depth parameter C_{ZB} has been described by the linearized theory. If such a bulb of constant volume and longitudinal position is moved form infinite depth up to the water surface, the interferential effect increases at first monotonically from zero to a maximum, decreases subsequently, and finally become negative due to an increase of the resistance of the emerging bulb body.

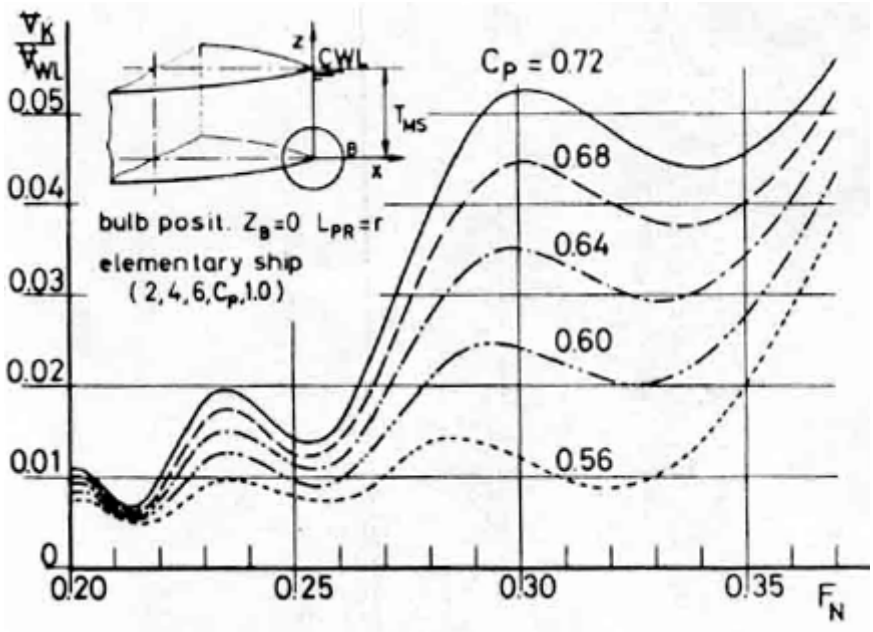

Fig 4.9 Optimum Bulb Volume of Ship-Bulb Combination as a function of Fn

4.5.3 Optimum Bulb Volume V_K

Mass Volume of the ship V_{WL} = 210382.4 m^3

From the graph, for the Fn = 0.213 and C_P = 0.674,

$$V_K/V_{WL} = 0.008$$

Hence, V_K = 1683.06 m^3

4.5.4 Bulb Resistance

Referring to Equation 18, the total wave resistance coefficient of the ship can be split with an extra term called bulb resistance coefficient for the bulb performance analysis. This is done to isolate the bulb from the hull and to calculate the wave resistance for the bulb alone. The surface area and the bulb volume will play a major role in the wave formation around the hull. The amplitude function is substituted in the Michelle's equation to calculate the bulb wave

resistance and finally to calculate the wave resistance coefficient.

$$C_W = C_{HULL} + C_{BULB}$$

Mitchelle's integral is computed in Mathematica 4.1 software for limits $-\pi/2$ to $\pi/2$ and the results are shown in the graph below.

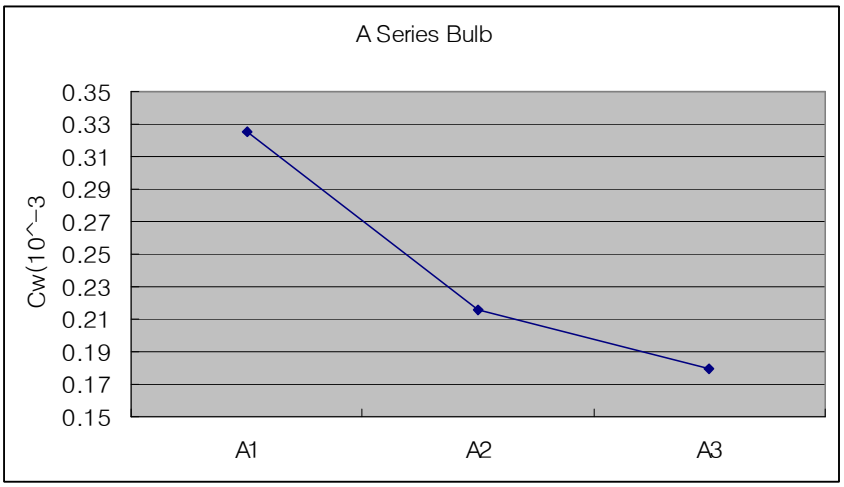

Fig 4.10 Bulb Coefficient for 'A' Series Bulb

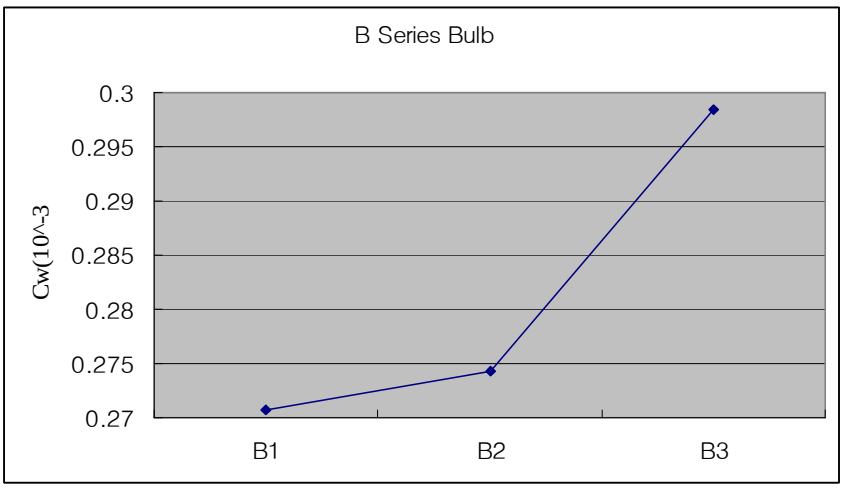

Fig 4.11 Bulb Coefficient for 'B' Series Bulb

4.5.5 Power Reduction

Since the bulbous bow affects primarily the wave making resistance, the design guidelines should correctly b related to the wave or residual resistance. In this theory, the bulb effect is derived from resistance or propulsion tests or a power specific bulb power reduction factor [1]:

$$\Delta P^* = 1.0 - P_W/P_o \tag{19}$$

In this form, the bulb effect is the power difference of the ship with out P_0 and with bulb P_W related to the power of the bulbless ship. According to the theory, a positive bulb effect corresponds to a power reduction overall and vise versa.

In order to separate the different friction resistance component of the ship with and with out bulb in accordance with Froude's method, the total delivered power, P_D is split into residuary part P_R and frictional part P_F respectively. From the propulsive efficiency η_D, the residuary power can be can be calculated as the difference between total and frictional power, and the residuary reduction factor

$$\Delta P^*_R = 1.0 - \frac{P_{DW} - P_{FW}}{P_{D0} - P_{F0}} \tag{20}$$

can be defined.

The relationship between effective power P_E and the delivered power is

$$P_D = \frac{P_E}{\eta_D} = \frac{P_{ER} - P_{EF}}{\eta_D} \tag{21}$$

With the frictional power P_{EF} calculated by International Towing Tank Conference (ITTC) 1957 line, the residual power is

$$P_R = \frac{P_{ER}}{\eta_D} = P_D - \frac{P_{EF}}{\eta_D} \tag{22}$$

Form the equations 16-18, the residual power reduction factor becomes

$$\Delta P^*_R = 1.0 - \frac{p_{DW}\eta_{DW} - P_{EFW}}{P_{D_0}\eta_{D0} - P_{EF0}} x \frac{\eta_{D0}}{\eta_{DW}} \tag{23}$$

The propulsive efficiency η_D is a function of hull form and speed and for the ships without and with bulb, the propulsive efficiencies are generally not equal, but it is little greater in the beneficial speed range of the bulb ship. But for the calculations here, it is assumed that both the values nearly coincide.

For the calculation of total power delivered, a dimensionless coefficient $C_{P\nabla}$ is introduced and the coefficient is split into residuary and frictional terms. The residual power coefficient is given by

$$C_{p\nabla R} = \frac{P_D}{0.5\rho V_S^{\ 3}\sqrt[3]{\nabla_{WL}^{\ 2}}} - \frac{C_F S}{\eta_D \sqrt[3]{\nabla^2_{WL}}} \tag{24}$$

And C_F is evaluated by the ITTC 1957 Formula:

$$C_F = \frac{0.075}{(\log R_n - 2)^2} \tag{25}$$

The residual power coefficient is a function of Froude number and bulb form. The whole calculations for the power reduction calculation has been performed by comparing the hull form with a bulbless ship with the same displacement and block coefficient. If the delivered power for the bulbless ship is known, then the required power for the bulb ship can be calculated by the formula given below.

$$P_D = \{(1.0 - \Delta C_{P\nabla R})C_{P\nabla R_0} + (\frac{C_F S}{\eta_D \sqrt[3]{\nabla_{WL}^{\ 2}}})\}\frac{\rho}{2} V_S^{\ 3} \sqrt[3]{\nabla^2_{WL}} \quad (26)$$

Where $C_{P\nabla R0}$ is the residual power coefficient for a bulbless ship. Residuary power reduction coefficient $\Delta C_{P\nabla R}$ is calculated form the graph results of fig (4.10) as a function of length parameter.

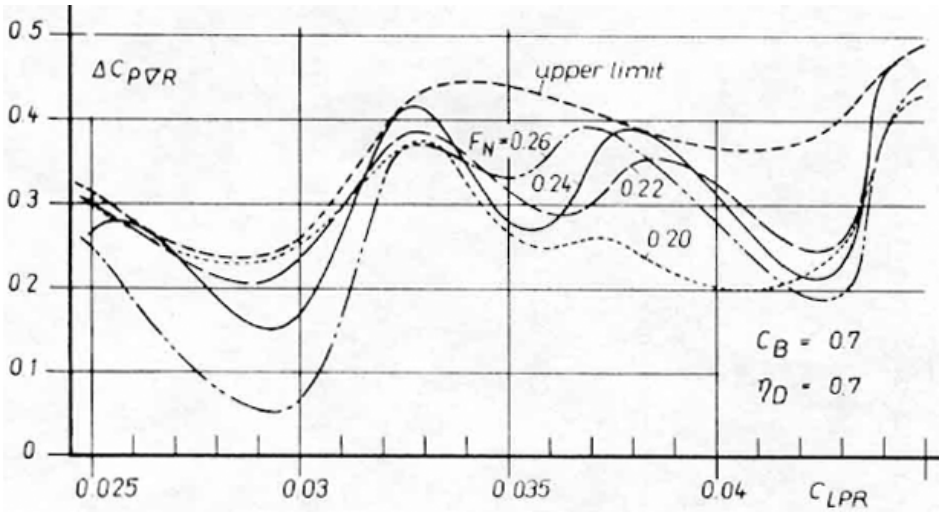

Fig 4.12 Residual Power Reduction Coefficient as a function of Length Parameter

Table 4.3 Residual Power Coefficient Calculation for Bulbless Hull

V	Fn	Cr(10^{-3})	C_F(10^{-3})	P_D(kW)	$C_{P\nabla ro}$
26	0.221693	2.93	1.39	101592.6	0.009784
25.5	0.21743	2.82	1.40	95544.12	0.009679
25	0.213167	3.14	1.44	92515.42	0.009951
24.5	0.208903	2.96	1.40	85438.62	0.009805
24	0.20464	2.66	1.41	79501.47	0.009523

23	0.196113	1.68	1.42	67468.84	0.008604
22	0.187587	1.69	1.42	59263.56	0.008608
21	0.17906	1.34	1.43	50979.34	0.008276
20	0.170533	1.03	1.44	43631.7	0.007976
19	0.162007	7.74	1.45	37159.78	0.007736

Now for the range of speed specified above, the Delivered power calculation followed by

Effective power calculation is done with reference to the bulbless ship values.

Table 4.4 Power Calculation for A1 Bulb

V	**Fn**	**∇Cp∇r**	**Cr(10^{-3})**	**Cf(10^{-3})**	**Cp∇ro**	**Pd(kW)**	**P_E(kW)**
26	0.23	0.14	4.80	1.387	0.009784	96930.09	67851.07
25.5	0.22	0.139	6.09	1.391	0.009679	91280.88	63896.62
25	0.21	0.13	2.61	1.394	0.009951	87380.14	61166.1
24.5	0.209	0.125	3.37	1.397	0.009805	82066.86	57446.8
24	0.205	0.11	5.00	1.401	0.009523	76925.71	53848
23	0.196	0.11	4.70	1.408	0.008604	65463.11	45824.18
22	0.188	0.109	3.52	1.416	0.008608	57533	40273.1
21	0.179	0.105	4.61	1.424	0.008276	49622.77	34735.94
20	0.171	0.1048	3.64	1.433	0.007976	42518.08	29762.65
19	0.162	0.104	4.45	1.442	0.007736	36253.66	25377.56

Table 4.5 Power Calculation for A2 Bulb

V	Fn	∇Cp∇r	Cr(10^{-3})	Cf(10^{-3})	Cp∇ro	Pd(kW)	P_E(kW)
26	0.23	0.28	4.38	1.39	0.009784	91040.31	63728.21
25.5	0.22	0.276	5.90	1.39	0.009679	85862	60103.4
25	0.21	0.265	4.32	1.39	0.009951	82207.33	57545.13
24.5	0.209	0.259	5.06	1.40	0.009805	77341.99	54139.4
24	0.205	0.25	2.03	1.40	0.009523	72384.14	50668.9
23	0.196	0.243	3.29	1.41	0.008604	62062.31	43443.61
22	0.188	0.2355	4.38	1.42	0.008608	54676.19	38273.33
21	0.179	0.228	2.70	1.42	0.008276	47323.11	33126.18
20	0.171	0.2205	4.50	1.43	0.007976	40699.4	28489.58
19	0.162	0.213	3.37	1.44	0.007736	34829.12	24380.38

Table 4.6 Power Calculation for A3 Bulb

V	Fn	∇Cp∇r	Cr(10^{-3})	Cf(10^{-3})	Cp∇ro	Pd(kW)	P_E(kW)
26	0.23	0.39	3.61	1.38	0.009784	86380.38	60466.27
25.5	0.22	0.379	4.40	1.39	0.009679	81790.45	57253.32
25	0.21	0.364	2.86	1.43	0.009951	79776.8	55843.76
24.5	0.209	0.341	3.70	1.39	0.009805	74432.75	52102.92
24	0.205	0.33	1.28	1.40	0.009523	69827.75	48879.43
23	0.196	0.3134	2.52	1.41	0.008604	60250.2	42175.14

22	0.188	0.2976	2.98	1.41	0.008608	53304.43	37313.1
21	0.179	0.2818	1.83	1.42	0.008276	46311.33	32417.93
20	0.171	0.266	4.40	1.43	0.007976	40008.01	28005.61
19	0.162	0.2502	2.00	1.44	0.007736	34363.76	24054.63

Table 4.7 Power Calculation for B1 Bulb

V	Fn	▽Cp▽r	Cr(10^{-3})	Cf(10^{-3})	Cp▽ro	Pd(kW)	P_E(kW)
26	0.23	0.285	4.13	1.39	0.009784	90753.11	63527.17
25.5	0.22	0.283	5.10	1.39	0.009679	85514	59859.8
25	0.21	0.279	3.55	1.43	0.009951	82920.87	58044.61
24.5	0.209	0.275	4.46	1.40	0.009805	76709.66	53696.76
24	0.205	0.27	1.95	1.40	0.009523	71709.62	50196.73
23	0.196	0.267	2.72	1.41	0.008604	61390.73	42973.51
22	0.188	0.2632	3.41	1.41	0.008608	54004.44	37803.11
21	0.179	0.2594	2.60	1.42	0.008276	46666.98	32666.88
20	0.171	0.2556	4.28	1.43	0.007976	40092.98	28065.09
19	0.162	0.2518	2.39	1.43	0.007736	34121.91	23885.34

Table 4.8 Power Calculation for B2 Bulb

V	Fn	▽Cp▽r	Cr(10^{-3})	Cf(10^{-3})	Cp▽ro	Pd(kW)	P_E(kW)
26	0.23	0.245	2.02	1.38	0.009784	92360.66	64652.46
25.5	0.22	0.236	3.02	1.39	0.009679	87290.77	61103.54

25	0.21	0.221	1.51	1.42	0.009951	84991.2	59493.84
24.5	0.209	0.214	2.01	1.39	0.009805	78805.92	55164.14
24	0.205	0.205	1.34	1.40	0.009523	73751.12	51625.78
23	0.196	0.1936	0.25	1.40	0.008604	63224.28	44256.99
22	0.188	0.1834	1.07	1.41	0.008608	55781.3	39046.91
21	0.179	0.1732	0.23	1.42	0.008276	48272.82	33790.97
20	0.171	0.163	1.94	1.43	0.007976	41549.72	29084.8
19	0.162	0.1528	0.28	1.44	0.007736	35570.17	24899.12

Table 4.9 Power Calculation for B3 Bulb

V	**Fn**	**∇Cp∇r**	**Cr(10^{-3})**	**Cf(10^{-3})**	**Cp∇ro**	**Pd(kW)**	**P_E(kW)**
26	0.23	0.39	3.61	1.38	0.009784	86337.18	60436.03
25.5	0.22	0.371	4.86	1.39	0.009679	82066.86	57446.8
25	0.21	0.342	2.86	1.42	0.009951	80544.67	56381.27
24.5	0.209	0.326	3.29	1.39	0.009805	74931.28	52451.9
24	0.205	0.305	4.31	1.40	0.009523	70572.6	49400.82
23	0.196	0.2823	3.46	1.40	0.008604	61024.32	42717.02
22	0.188	0.2608	3.37	1.41	0.008608	54084.86	37859.4
21	0.179	0.2393	4.20	1.42	0.008276	47070	32949
20	0.171	0.2178	3.23	1.43	0.007976	40727.96	28509.57
19	0.162	0.1963	3.17	1.44	0.007736	35036.07	24525.25

CHAPTER 5

SHIPFLOW ANALYSIS FOR BULBS

5.1 About SHIPFLOW

Applications of computational fluid dynamics (CFD) to the maritime industry continue to grow as this advanced technology takes advantage of the increasing speed of computers. Numerical approaches have evolved to a level of accuracy which allows them to be used during the design process to predict ship resistance. Significant progress has been made in predicting flow characteristics around a given ship hull. Ship designers can use this information to improve a ship's design. However, not much effort has been dedicated to determining viscous drag, an important element in the development of a new design. The final checking and analysis of the bulb design is done in the CFD module SHIPFLOW. The wave making and frictional resistance as well as the flow round the hull for various bulb shapes have been calculated using SHIPFLOW. The flow around a body can be described mathematically as a function of fluid pressure and the three components of velocity. A set of governing equations of motions can be created, like the Navier-Stokes equations for turbulent flow, and solved in association with specific boundary conditions. These equations are often complex to solve and rely on the use of Computational Fluid Dynamics (CFD). SHIPFLOW is a CFD tool specifically developed to solve marine related problems (SHIPFLOW, 1999). To investigate the flow around a ship or ship model, SHIPFLOW splits the flow into three regions, shown in Figure below; the region of potential flow, which neglects viscous effects and is associated with the wave-making

pattern, the region of boundary-layer flow and the region where the complete Navier-Stokes equations are solved.

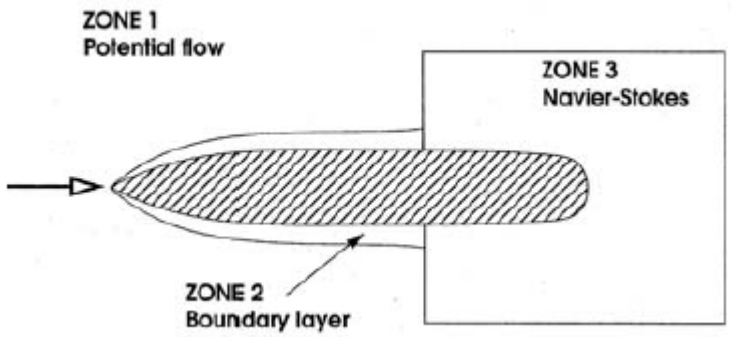

Fig 5.1 The different flow regions assumed by SHIPFLOW

In CFD analyses of marine vehicles, it is customary to use **i**, **j**, and **k** to describe the grid dimensions, where **i**-direction is in the axial direction, **j** is normal to the body, and **k** is around the body's girth.

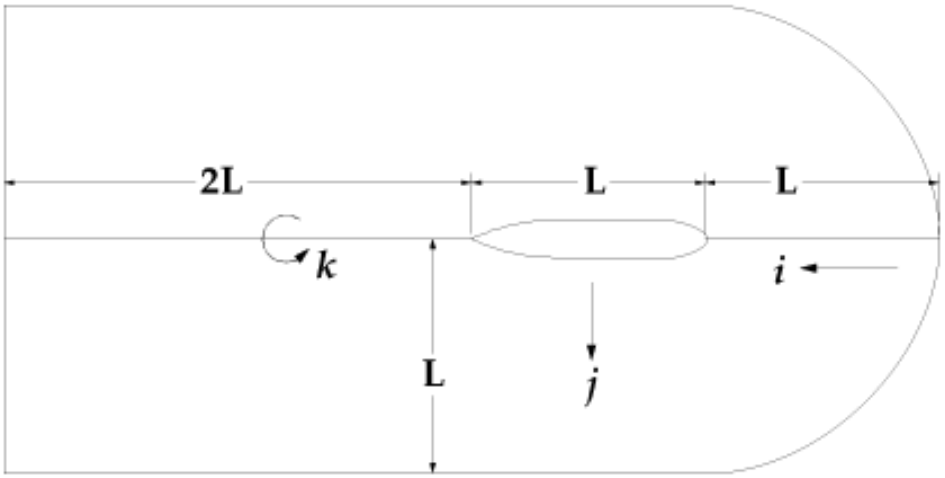

Figure 5.2 Schematic of grid structure around an axis-symmetric body

The following potential flow techniques are used in Zone 1 to predict pressures, velocities and streamlines. By assuming non-viscous (ideal) and irrotational flow the governing equations produced are the linear, partial differential Laplace equations based on mass continuity. The non-linear free-surface boundary conditions are linearized and solved by using an iterative process until satisfactory convergence is reached.

In Zone 2 the development of the boundary layer is investigated using momentum integral equations for the thin viscous layer along the hull. By ignoring cross flow in the boundary layer, which is created due to a pressure gradient in the vertical direction of the ship hull the results are ordinary differential equations which are solved by Runge-Kutta techniques. This prediction cannot be used at the stern of a ship where a thick viscous region occurs due to convergence of the streamlines. Towards the stern of the vessel, Reynolds-averaged Navier-Stokes (RANS) equations along with mass continuity equations describe the flow in Zone 3. The solution of the complex Navier-Stokes equations requires a lot of computational time and is therefore restricted to the stern of the vessel only, where a denser panelisation is created. The unsteadiness of the turbulent region is averaged out and instantaneous values of pressure and velocity are separated into a mean with fluctuations by the introduction of Reynolds stresses.
The programming is split into six modules and SHIPFLOW considers each module at a time. The method is unidirectional, in other words the results of the last module do not affect, for example, the second module. These six modules are listed below, in the order in which SHIPFLOW assesses them.

5.1.1 XFLOW

Defines the general physical properties of the surroundings, for example the fluid, characteristics, initial ship position, ship speed, etc..

5.1.2 XMESH

Using the information from XFLOW, XMESH generates the panelisation of the free surface and the vessel for use by the third module XPAN. The model can be viewed in the post processor.

5.1.3 XPAN

XPAN computes the potential flow around the model (i.e. Zone 1) and free-surface, which are made up of quadrilateral panels each containing Rankine sources. XPAN can operate under linear or non-linear free-surface boundary conditions. Results obtained from XPAN are displayed by the post processor and listed in output files. The results include wave-making coefficient (CW), wave pattern, potential streamlines, pressure and velocity contours.

5.1.4 XBOUND

XBOUND is concerned with the thin turbulent boundary layer surrounding the hull (i.e. Zone 2). Using momentum integral equations SHIPFLOW provides the frictional resistance coefficient (CF), boundary layer thickness ™, as well as other parameters associated with the boundary layer.

5.1.5 XGRID

XGRID generates the grid towards the stern of the vessel used to represent Zone 3 where the Navier-Stokes equations describe the fluid flow.

5.1.6 XVISC

The final module of SHIPFLOW solves the Reynolds-averaged Navier-Stokes equations. XVISC provides the viscous pressure resistance coefficient (CVP) and therefore the total resistance CT can be estimated. XVISC can also be used to investigate the wake and values such as axial, radial and tangential velocities at various planes towards the stern are obtained.

The frictional, wave and total resistance coefficients as computed by SHIPFLOW, together with the total resistance as measured from the experiments and the Schoenherr and ITTC ship-model correlation lines. The well-known equations for the ITTC and Schoenherr lines are respectively:

$$C_F = 0.075/(\log(Re)-2)^2$$
$$0.242/C_F^{0.5} = \log(ReC_F) \qquad (27)$$

5.1.7 Theory

The normal Rankine source equation is employed in calculating the wave resistance taking into consideration the Viscous effect at the aft region. For a fixed coordinate system oxyz with origin at O at the intersection of the midship section and the undisturbed free surface, the Rankine Source Equation is defined as follows.

$$\Phi(x, y, z) = Ux + \iint_S \left(\frac{\sigma(q)}{r(p,q)}\right) ds \qquad (28)$$

Where σ is the source density and r is the distance from the integration point q(x', y', z') on S to point p(x, y, z) and the surface S is divided into quadrilateral panels.

5.2 SHIPFLOW Analysis and Results

The calculation has been performed in view of a comparative study of each bulb shapes with respect to the bulbless hull. The hull input parameters include the block coefficient, Froude number and Reynolds number in the command file. The different hull offsets are manually made for varying bulb shape according to the study and is analyzed separately for a range of Froude numbers.

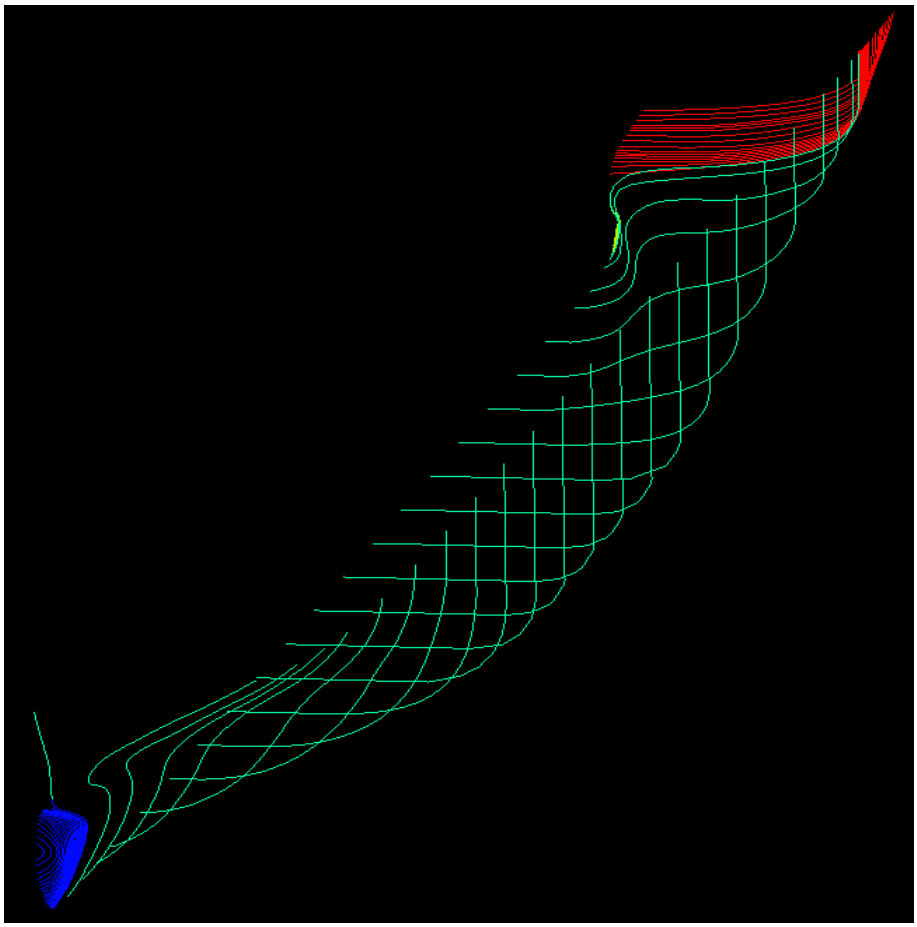

Fig 5.3 The Panel Offset Lines for the SHIPFLOW

5.2.1 Resistance Calculation

The wave making and frictional coefficient is calculated from SHIPFLOW output and the rest of the calculations to compute the power is done by 3-Dimesional formula

$$C_T = C_W + C_F(1+K) + C_{AA} + \Delta C_F \quad (29)$$

where C_W is the wave making resistance coefficient, C_F is the frictional resistance coefficient, C_{AA} is the air resistance coefficient and K is the form factor.

Table 5.1 A1 Bulb: Effective Power Calculation (Ship flow Results)

Fn	Rn	Cr(10^{-3})	Cf(10^{-3})	Caa(10^{-3})	Ct(10^{-3})	Rt(kW)	PE(kW)
0.222	3.798E+09	3.80	1.387	1.50	6.687	5208.87	69665.50
0.217	3.725E+09	4.09	1.391	1.50	6.981	5025.52	65920.70
0.213	3.652E+09	2.11	1.394	1.50	5.004	4795.04	61664.28
0.209	3.579E+09	2.37	1.397	1.50	5.267	4616.55	58181.48
0.205	3.506E+09	3.00	1.401	1.50	5.901	4546.79	56132.80
0.196	3.360E+09	3.47	1.408	1.50	6.378	4178.88	49441.13
0.188	3.214E+09	3.02	1.416	1.50	5.936	3845.49	43518.67
0.179	3.068E+09	3.31	1.424	1.50	6.234	3520.01	38024.55
0.171	2.922E+09	3.14	1.433	1.50	6.073	3202.64	32948.71
0.162	2.776E+09	3.45	1.442	1.50	6.392	2856.60	27919.31

Table 5.2 A2 Bulb: Effective Power Calculation (Ship flow Results)

Fn	Rn	Cr(10^{-3})	Cf(10^{-3})	Caa(10^{-3})	Ct(10^{-3})	Rt(kW)	PE(kW)
0.222	3.798E+09	3.38	1.39	1.50	6.27	4699.95	62858.97
0.217	3.725E+09	3.90	1.39	1.50	6.79	4558.28	59791.90
0.213	3.652E+09	3.82	1.39	1.50	6.71	4350.82	55951.61
0.209	3.579E+09	4.06	1.40	1.50	6.96	4260.72	53696.98
0.205	3.506E+09	4.03	1.40	1.50	6.93	4040.14	49878.01
0.196	3.360E+09	4.52	1.41	1.50	7.43	3812.98	45112.11
0.188	3.214E+09	4.88	1.42	1.50	7.8	3489.58	39490.87
0.179	3.068E+09	4.00	1.42	1.50	6.92	3166.33	34203.91
0.171	2.922E+09	4.00	1.43	1.50	6.93	2857.23	29395.23
0.162	2.776E+09	4.37	1.44	1.50	7.31	2615.05	25558.45

Table 5.3 A3 Bulb: Effective Power Calculation (Ship flow Results)

Fn	Rn	Cr(10^{-3})	Cf(10^{-3})	Caa(10^{-3})	Ct	Rt(kW)	PE(kW)
0.222	3.798E+09	1.02	1.38	1.50	3.9	5021.64	67161.42
0.217	3.725E+09	1.02	1.39	1.50	3.91	4774.35	62626.11
0.213	3.652E+09	1.01	1.43	1.50	3.94	4674.04	60108.18
0.209	3.579E+09	1.01	1.39	1.50	3.9	4494.15	56638.86
0.205	3.506E+09	1.34	1.40	1.50	4.24	4422.55	54599.07
0.196	3.360E+09	1.48	1.41	1.50	4.39	3986.85	47169.24

0.188	3.214E+09	1.57	1.41	1.50	4.48	3619.32	40959.14
0.179	3.068E+09	1.53	1.42	1.50	4.45	3261.32	35230.09
0.171	2.922E+09	1.44	1.43	1.50	4.37	2927.28	30115.82
0.162	2.776E+09	1.28	1.44	1.50	4.22	2567.59	25094.59

Table 5.4 B1 Bulb: Effective Power Calculation (Ship flow Results)

Fn	Rn	Cr(10^{-3})	Cf(10^{-3})	Caa(10^{-3})	Ct	Rt(kW)	PE(kW)
0.222	3.798E+09	3.13	1.39	1.50	6.02	4925.95	65881.61
0.217	3.725E+09	3.10	1.39	1.50	5.99	4717.33	61878.17
0.213	3.652E+09	3.05	1.43	1.50	5.98	4615.57	59356.23
0.209	3.579E+09	3.46	1.40	1.50	6.36	4452.60	56115.23
0.205	3.506E+09	3.95	1.40	1.50	6.85	4367.97	53925.17
0.196	3.360E+09	3.95	1.41	1.50	6.86	4022.69	47593.29
0.188	3.214E+09	3.91	1.41	1.50	6.82	3685.03	41702.75
0.179	3.068E+09	3.90	1.42	1.50	6.82	3366.94	36371.00
0.171	2.922E+09	3.78	1.43	1.50	6.71	3048.80	31366.05
0.162	2.776E+09	3.39	1.43	1.50	6.32	2708.76	26474.34

Table 5.5 B2 Bulb: Effective Power Calculation (Ship flow Results)

Fn	Rn	Cr(10^{-3})	Cf(10^{-3})	Caa(10^{-3})	Ct	Rt(kW)	PE(kW)
0.222	3.798E+09	2.61	1.38	1.50	3.9	4786.90	64021.95
0.217	3.725E+09	2.40	1.39	1.50	3.91	4567.77	59916.35
0.213	3.652E+09	2.36	1.42	1.50	3.93	4524.29	58182.42
0.209	3.579E+09	2.70	1.39	1.50	3.9	4362.95	54985.34
0.205	3.506E+09	3.28	1.40	1.50	4.24	4305.52	53154.17
0.196	3.360E+09	3.75	1.40	1.50	4.38	3955.89	46802.98
0.188	3.214E+09	3.48	1.41	1.50	4.48	3629.88	41078.64
0.179	3.068E+09	3.13	1.42	1.50	4.45	3312.89	35787.13
0.171	2.922E+09	3.90	1.43	1.50	4.37	3004.95	30914.95
0.162	2.776E+09	3.00	1.44	1.50	4.22	2665.14	26047.99

Table 5.6 B3 Bulb: Effective Power Calculation (Ship flow Results)

Fn	Rn	Cr(10^{-3})	Cf(10^{-3})	Caa(10^{-3})	Ct	Rt(kW)	PE(kW)
0.222	3.798E+09	2.61	1.38	1.50	5.49	4780.46	63935.85
0.217	3.725E+09	2.86	1.39	1.50	5.75	4689.55	61513.82
0.213	3.652E+09	2.36	1.42	1.50	5.28	4530.83	58266.48
0.209	3.579E+09	2.29	1.39	1.50	5.18	4220.51	53190.20
0.205	3.506E+09	2.31	1.40	1.50	5.21	4091.16	50507.87
0.196	3.360E+09	2.23	1.40	1.50	5.13	3720.29	44015.48

0.188	3.214E+09	2.87	1.41	1.50	5.78	3400.26	38480.07
0.179	3.068E+09	2.90	1.42	1.50	5.82	3130.99	33822.22
0.171	2.922E+09	2.73	1.43	1.50	5.66	2885.94	29690.57
0.162	2.776E+09	2.17	1.44	1.50	5.11	2692.03	26310.81

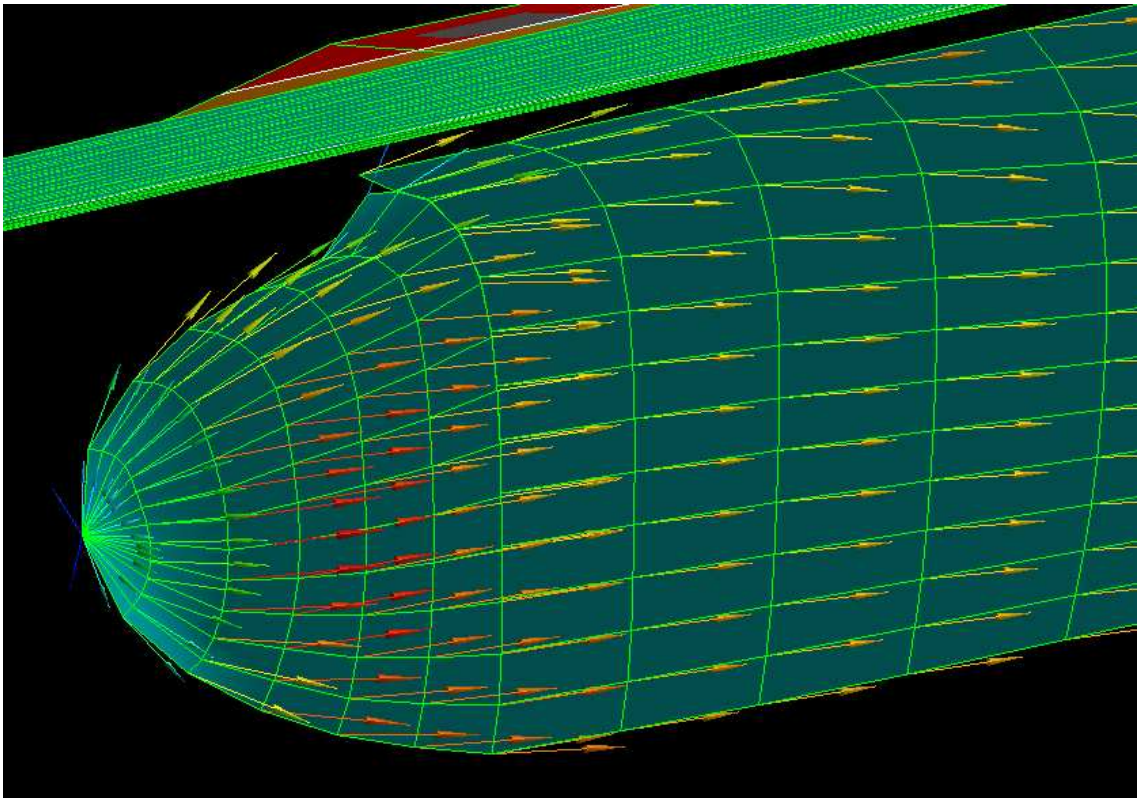

Fig 5.4 Flow Round the A1 Bulb

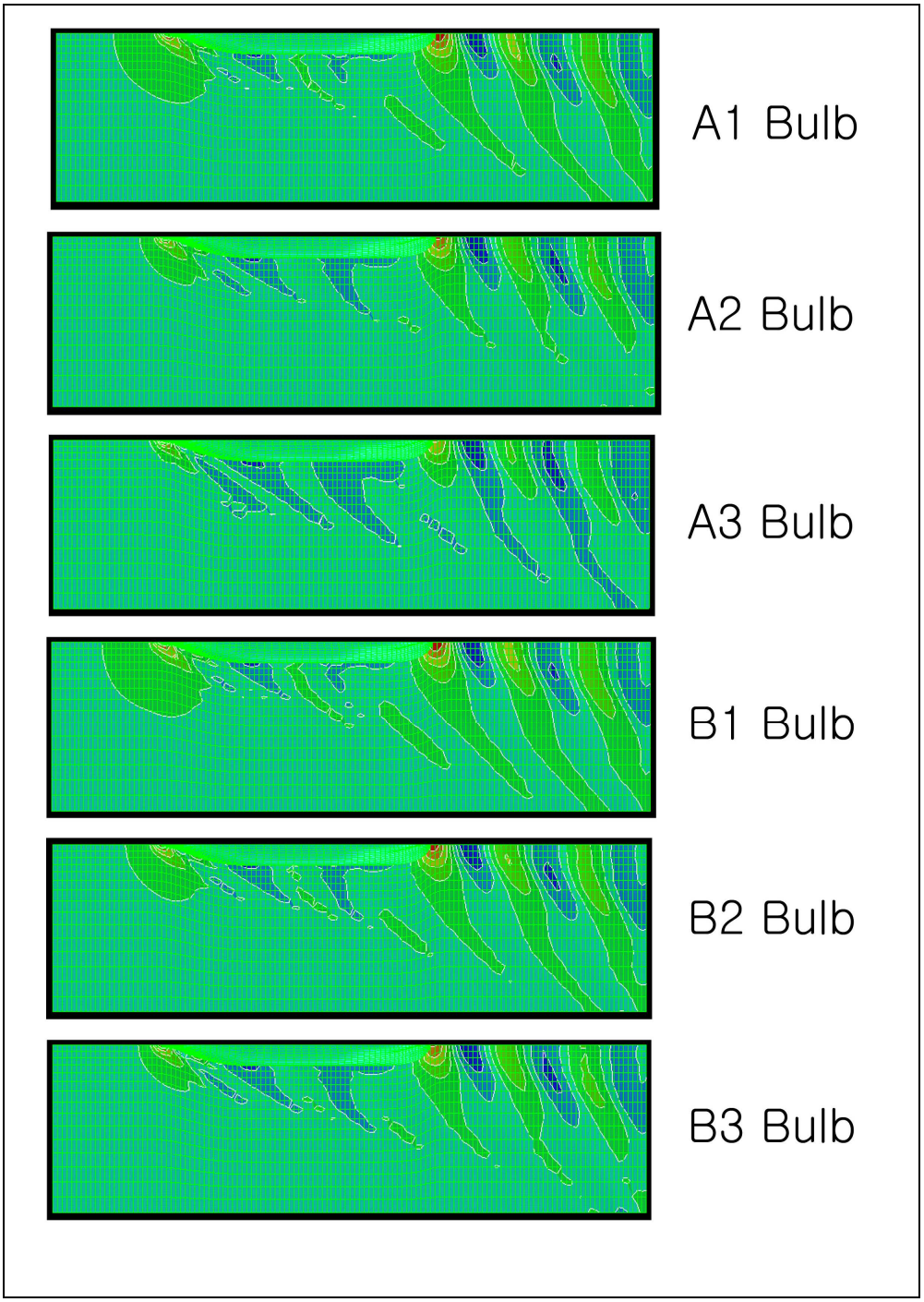

Fig 5.5 Wave Pattern for the Bulbs at 25 Knots from Ship flow

CHAPTER 6

COMPARATIVE STUDY

6.1 Wave Cut Analysis

Theoretical Wave-cut calculation performed and compared with the ship flow output for both 'A' series and 'B' series bulb sections and a correlative study is performed with respect to bulbless hull. The performance of bulb with respect to bulb cross section and nose height and its effect on hull is relevant from the wave cut diagrams. Each bulb appears to have different wave height at the fore perpendicular and Wave Ht/ L_{PP} is taken as a measure to assess the bulb performance. A3 bulb has been found to have a smooth wave profile with respect to other bulbs in the lot.

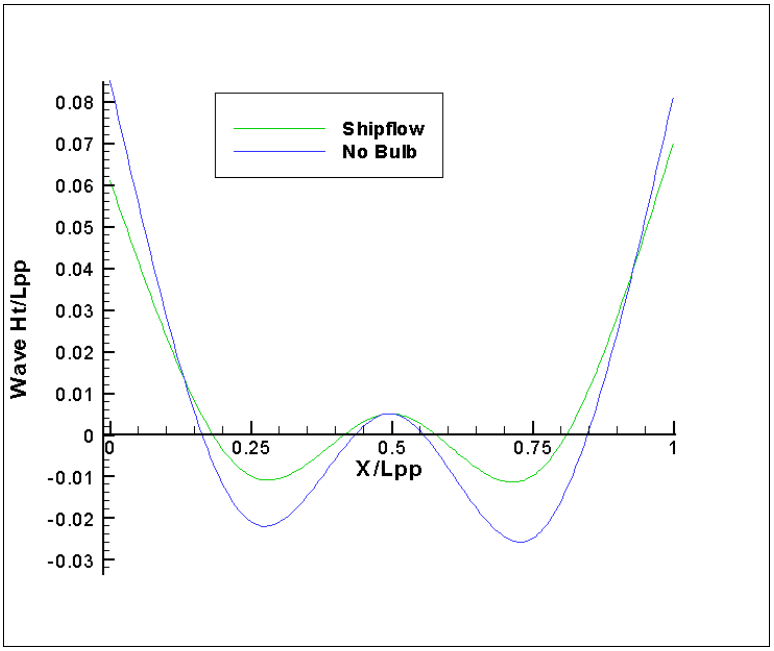

Fig 6.1 Wave cut for A1 Bulb

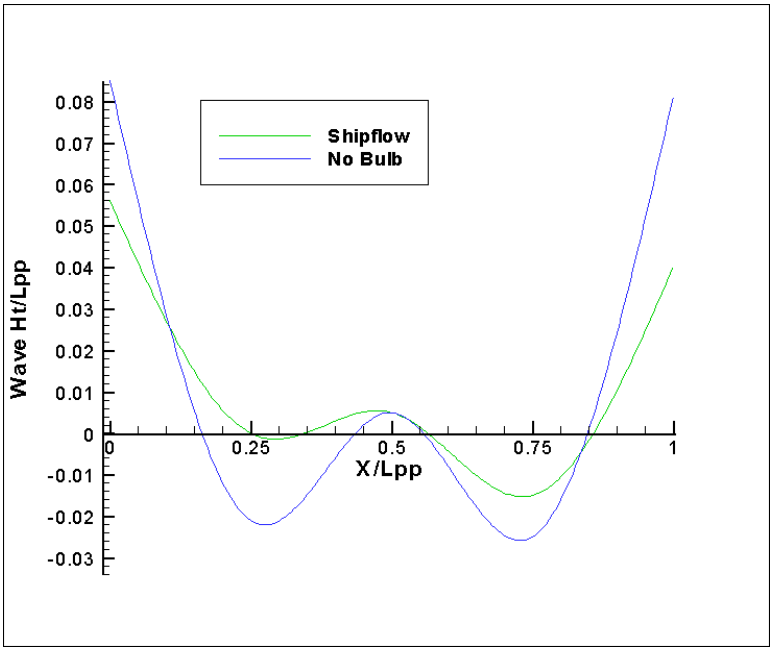

Fig 6.2 Wave cut for A2 Bulb

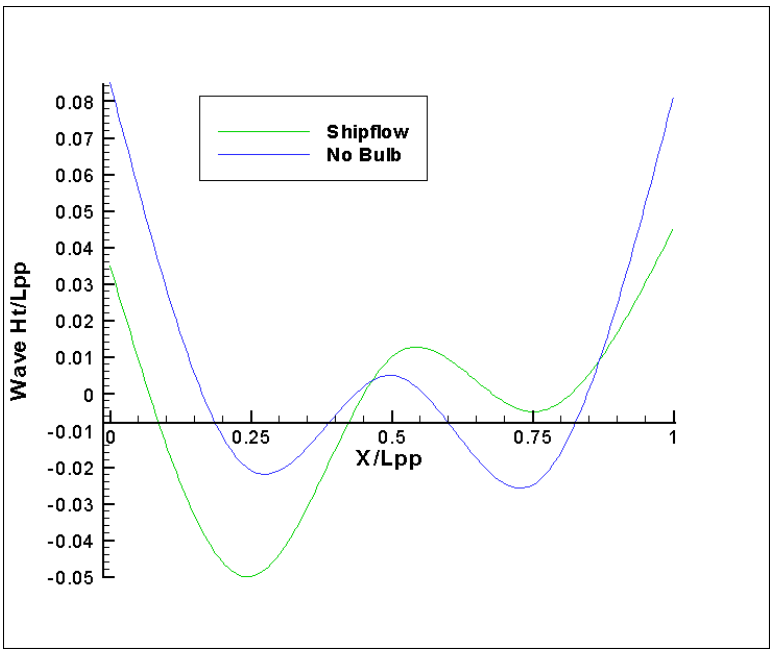

Fig 6.3 Wave cut for A3 Bulb

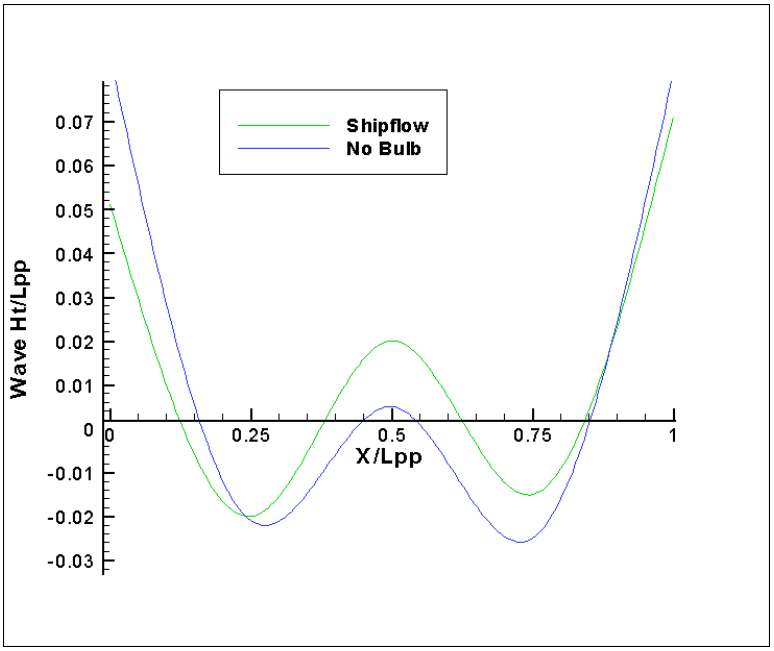

Fig 6.4 Wave cut for B1 Bulb

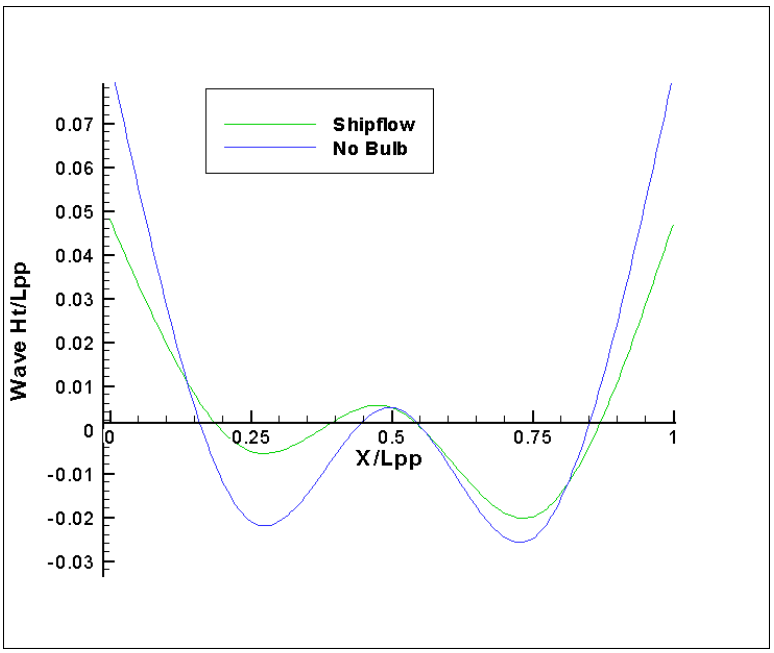

Fig 6.5 Wave cut for B2 Bulb

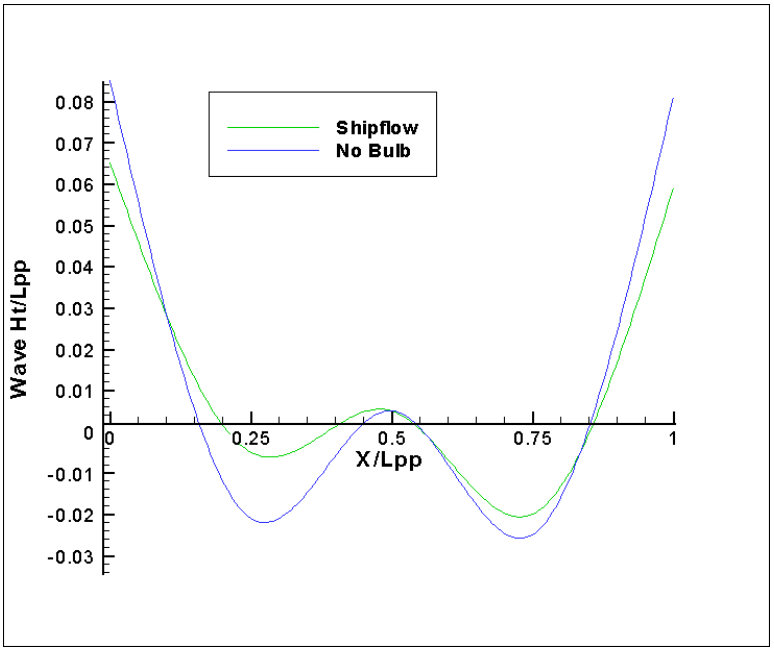

Fig 6.6 Wave cut for B3 Bulb

6.2 Power Calculation Comparison by Kracht Formula and SHIPFLOW

The Kracht method relies on the basic ITTC 1957 formula to calculate the frictional resistance. This method prescribes the Guldhammer and Harvard method to calculate the Wave making resistance with respect to prismatic coefficient and $L/\nabla^{1/3}$ values. The SHIPFLOW and Kracht method results for power are calculated for different bulb shapes and plotted from figs 6.7-6.12. This calculation is mainly done to assess and compare the power results of LR designed ULCS for the same capacity and the hull form designed for the study.

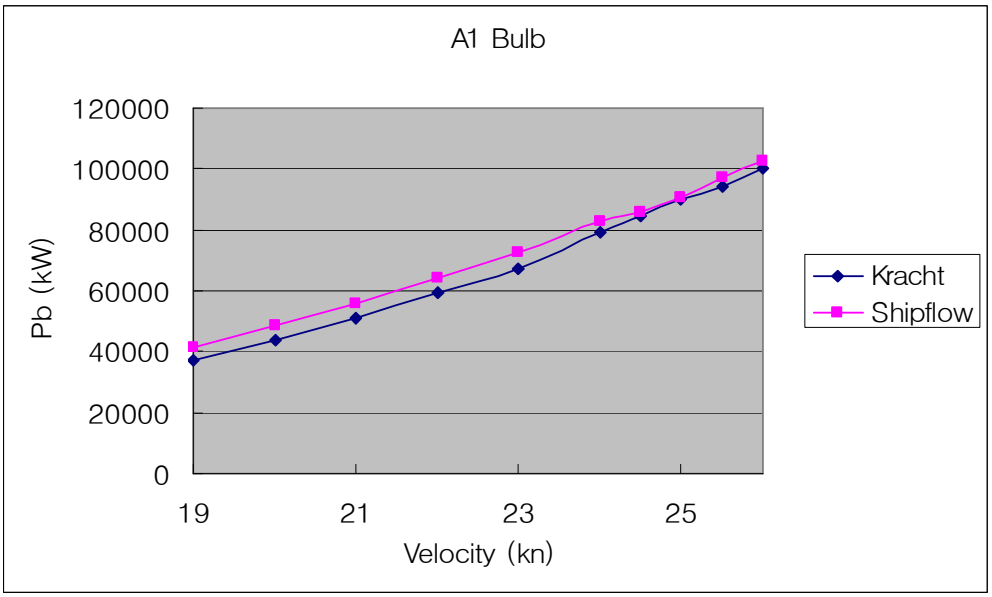

Fig 6.7 Power Curve for A1 Bulb

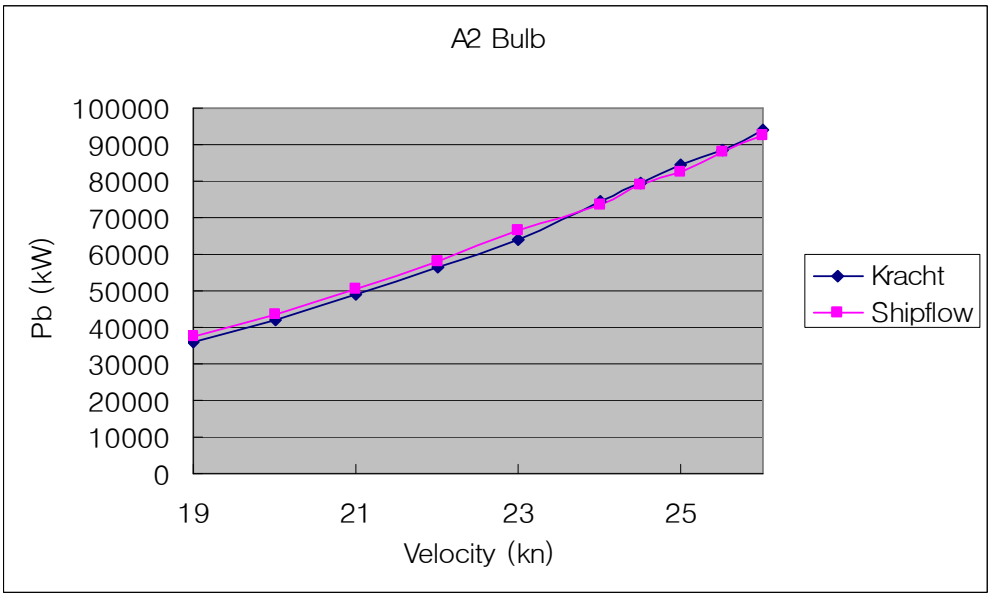

Fig 6.8 Power Curve for A2 Bulb

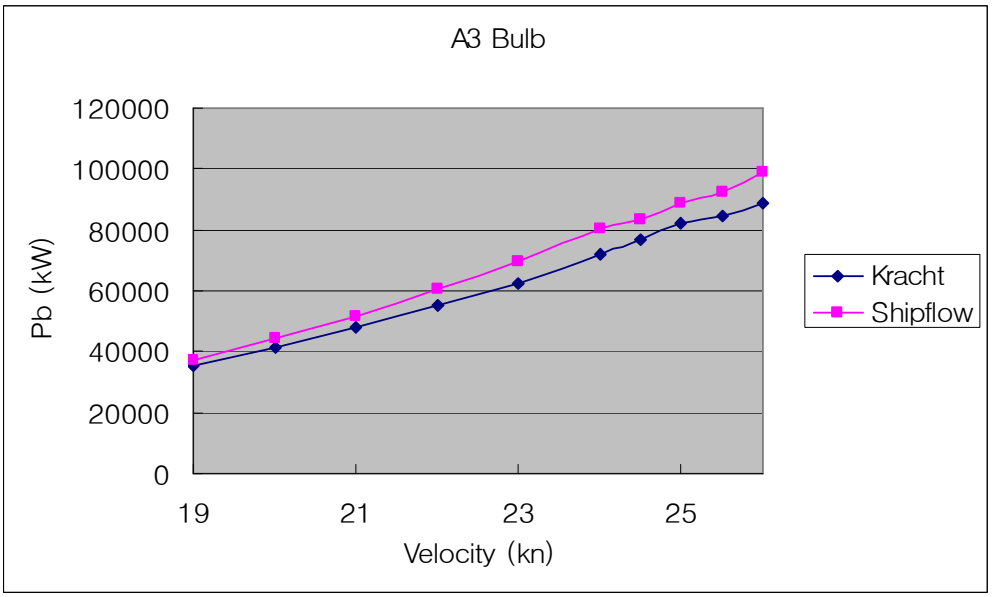

Fig 6.9 Power Curve for A3 Bulb

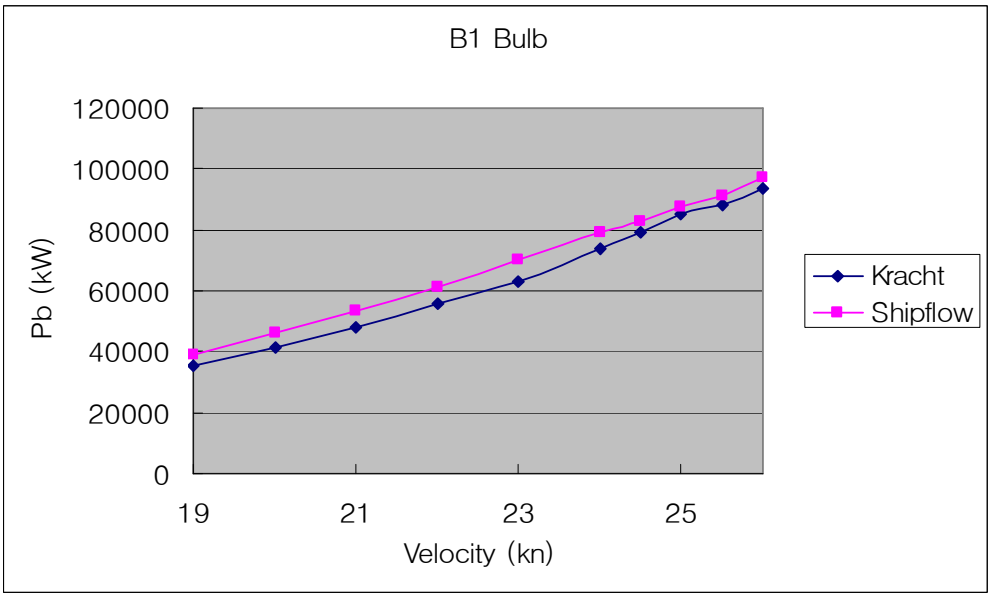

Fig 6.10 Power Curve for B1 Bulb

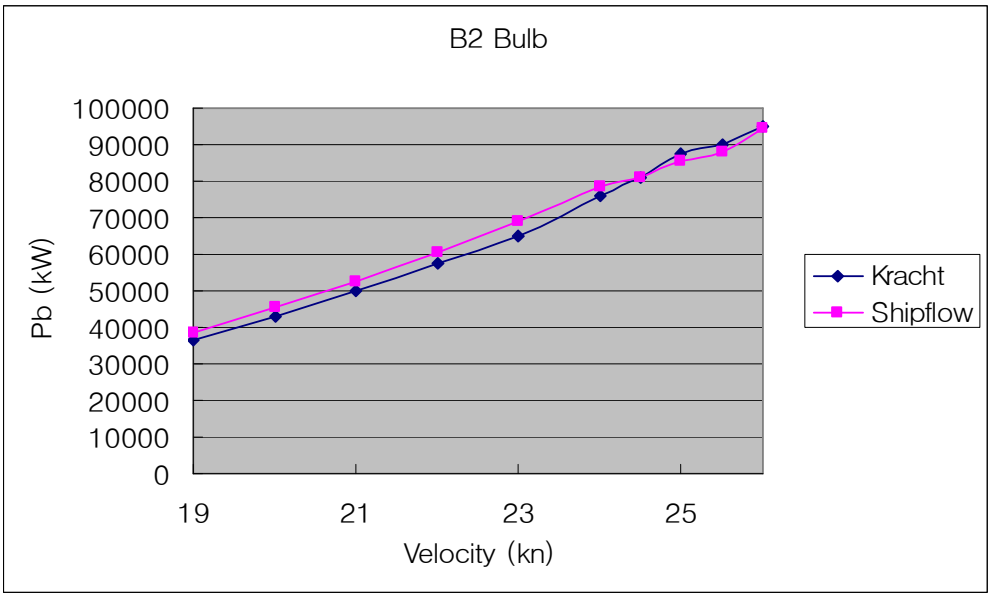

Fig 6.11 Power Curve for B2 Bulb

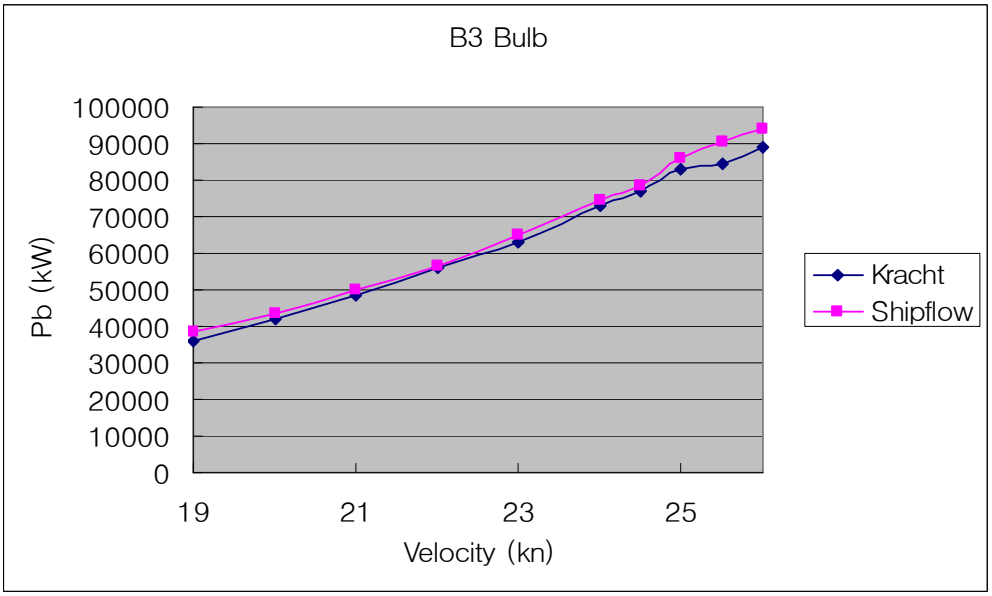

Fig 6.12 Power Curve for B3 Bulb

The results shows pretty close results with both the methods. At the design speed of 25 knots, the over all power calculated comes about 85MW. This result is in close account with the Lloyds calculation of power for the same capacity [8].

6.3 Optimum Area and Nose Height

Table 6.1 Bulb Parameters at 25 knots

Sec area varied	2.107	8.7	70.77
	3.819	8.9	90.43
	1.01	9.24	103.8
Nose Height varied	3.046	13.92	64.12
	2.36	12.325	82.34
	2.362	10.15	96.47

It's required to find an optimal value of the Nose height and Sectional area of the bulb at F.P. The value of optimum bulb area and nose height is calculated for minimum coefficient of wave making resistance. After interpolation, it's found that bulb of A3 cross section and a nose height of about 70% of the draft will yield a better performance as per the results.

6.4 Bulb Efficiency

The efficiency of each bulbs are compared with bulbless ship and efficiency of bulb is defines by the equation

$$\eta_D = \frac{P_{DO} - P_D}{P_D} \tag{30}$$

Where P_{DO} and P_D represents the power delivered for hull corresponding to different bulb shapes and bulbless ship respectively.

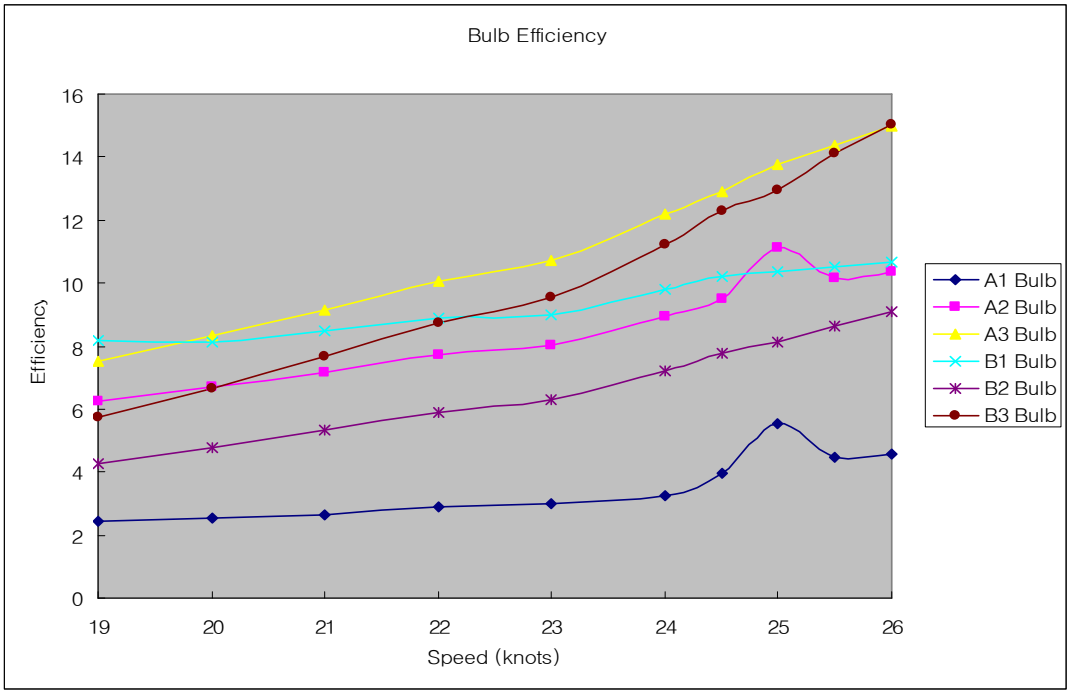

Fig 6.13 Bulb efficiency for 'A' & 'B' Series Bulb Shapes

Chapter 7

Conclusion

The overall study focuses on hull design and to find a proper blend of bulb shape for the mammoth hull shape. The two main challenges were to find the optimum speed and to achieve the power requirement with in the limits of the vessel. Hence the role played by the bulb shape is vital in reducing the overall resistance and effective power.

1) At the intended design speed of 25 knots, the over all power calculated for the engine is found to be around 85MW. This result is in close account with the Lloyds calculation (LR Technical Report, [8]) of power for the same capacity. Also the economic studies carried out in the first chapter also prove that the design speed of 25 knots is preferable and there is considerable reduction in container carrying cost.

2) All the bulb sections designed are analyzed in detail theoretically as well as computationally. When comparing a bulbless hull of same form coefficient with the bulbous forms, the bulb efficiencies are compared with respect to the power delivered. The efficiency of the two bulb series shows that the A3 bulb with the maximum cross sectional area and a high nose is much more effective from the resistance point of view.

3) Moreover, sharp low edge of the bulb enables the hull to resist slamming in heavy sea and to imbibe high speed characteristics. The Ray theory calculates the divergent waves generated and the entrance angle giving a theoretical insight into the desired wave pattern with a double source potential and shows that the A3 bulb shape is not generating any secondary waves and

have a minimum divergent wave angle.

4) The volume concentration and the centre of area for the A3 bulb at FP are also above the mean centre line of the bulb cross section. Hence there is a strong proof to conclude that out of the six bulb shape considered, A3 bulb comes out to have a pretty good blending with the hull form with very good hydrodynamic characteristics.

Overall layout of this study always stress for an optimum bulb shape that suitably fit to the hull form with an aim to smoothen the pressure distribution and finally the wave pattern around the hull.

Reference

[1] Alfred M Kracht, (1978). “Design of Bulbous Bows” *SNAME* Vol 86, pp 197-217

[2] Bohyun Yim, (1993). “The Selected Papers of Bohyun Yim”

[3] Bohyun Yim, (1993). “A Simple Design Theory and Method for Bulbous bows for Ships” *Journal of Ship Research*, Vol 18

[4] David Trozer (2003). “A review of Prospects for ultra-large Container ships and implications for the support fleet” *BOXSHIP 2003*

[5] Edward V Lewis, “Principle of Naval Architcture” *SNAME*

[6] Germanischer Lloyd (2001). “Development of Very Large Container Ships”

[7] Joseph B Keller, (1979). “The Ray Theory of Ships and Waves and the class of Stream lined Ships”, *J. Fluid Mech*, Vol 91, part 3, pp 465-488

[8] LR Technical Report (2001-2002). “Ultra Large Container Ships (ULCS)” Paper No: 5

[9] ShipFlow 2.4 Manual

[10] Sv. AA Harvald, “RESISTANCE AND PROPULSION OF SHIPS”

[11] Watson D.G.M & A.W.Gilfilan “Some Ship Design Methods” *RINA 76*

[12] Rules and regulations for Classification of Ships, Lloyds Register, 2003

[13] Sea Wave pattern Evaluation, E.O Tuck, L. Lazauskas & D.C Scullen, April 1999

Acknowledgement

A t the end of the day, it's my bounded duty to express my sincere gratitude and adoration to my Professor and Advisor Prof. Lee Kwi Joo for his incredible and impeccable support through out my study in Chosun University and finally to complete my Masters Thesis with great satisfaction. The support extended by Dr. Igor Shugan, visiting professor from Russia for my study is outstanding and I do remember him for his in depth knowledge in the subject and sense of humor. All other Professors namely Prof. Kwon Young Seob, Prof. Yoon Duck Young, Prof. Bang Han Sur, Prof. Joa Soon Won had been an excellent support and motivation for my entire study and I am deeply indebted to them too.

It's been a wonderful two years study in Chosun University and I had opportunity to study Korean Culture and Life style. I mixed well with my Korean friends and they let me feel good all the time. I also remember Miss Kim, Kyoung Hwa, Miss Park, Na Ra, Miss Lee, Eun Jung, Mr. Cho, Kyoung Hoon, Mr Lee, Sangbok and all my Indian friends for their timely help and support during arduous situations.

Finally, I strongly believe that the continual prayers and good gesture of my beloved parents back home are the root causes of my success and I do dedicate this thesis in their name. Above all, my prayers to '***The Almighty***' for a good beginning as a Naval Architect in near future.

저작물 이용 허락서

학 과	선박해양공학과	학 번	20037099	과 정	석사
성 명	한글: 사라스	한문 : 사라스	영문 : SARATH E.S		
주 소	광주광역시 동구 서석동 조선대학교 남백학기숙사 519 호				
연락처	E-MAIL : sarathes@yahoo.com				
논문제목	한글 : 초대형 컨테이너선의 구상선수 설계 영문 : A Study on the Bulbous Bow Design for Ultra Large Container Ship				

본인이 저작한 위의 저작물에 대하여 다음과 같은 조건아래 -조선대학교가 저작물을 이용할 수 있도록 허락하고 동의합니다.

- 다 음 -

1. 저작물의 DB 구축 및 인터넷을 포함한 정보통신망에의 공개를 위한 저작물의 복제, 기억장치에의 저장, 전송 등을 허락함
2. 위의 목적을 위하여 필요한 범위 내에서의 편집·형식상의 변경을 허락함. 다만, 저작물의 내용변경은 금지함.
3. 배포·전송된 저작물의 영리적 목적을 위한 복제, 저장, 전송 등은 금지함.
4. 저작물에 대한 이용기간은 5 년으로 하고, 기간종료 3 개월 이내에 별도의 의사표시가 없을 경우에는 저작물의 이용기간을 계속 연장함.
5. 해당 저작물의 저작권을 타인에게 양도하거나 또는 출판을 허락을 하였을 경우에는 1 개월 이내에 대학에 이를 통보함.
6. 조선대학교는 저작물의 이용허락 이후 해당 저작물로 인하여 발생하는 타인에 의한 권리 침해에 대하여 일체의 법적 책임을 지지 않음
7. 소속대학의 협정기관에 저작물의 제공 및 인터넷 등 정보통신망을 이용한 저작물의 전송·출력을 허락함.

2005 년 04 월 20 일

저작자: Sarath E.S (서명 또는 인)

조선대학교 총장 귀하